Matricellular Signaling Molecule CCN1 Attenuates Experimental Autoimmune Myocarditis by Acting as a Novel Immune Cell Migration Modulator

Madlen Rother, Stefanie Krohn, Gabriela Kania, Davy Vanhoutte, Andreas Eisenreich, Xiaomin Wang, Dirk Westermann, Kostas Savvatis, Nadine Dannemann, Carsten Skurk, Denise Hilfiker-Kleiner, Toni Cathomen, Henry Fechner, Ursula Rauch, Heinz-Peter Schultheiss, Stephane Heymans, Urs Eriksson, Carmen Scheibenbogen and Wolfgang Poller

Circulation. 2010;122:2688-2698; originally published online December 6, 2010;
doi: 10.1161/CIRCULATIONAHA.110.945261
Circulation is published by the American Heart Association, 7272 Greenville Avenue, Dallas, TX 75231

Print ISSN: 0009-7322. Online ISSN: 1524-4539

Matricellular Signaling Molecule CCN1 Attenuates Experimental Autoimmune Myocarditis by Acting as a Novel Immune Cell Migration Modulator

Madlen Rother, MSc*; Stefanie Krohn, MSc*; Gabriela Kania, PhD; Davy Vanhoutte, PhD; Andreas Eisenreich, PhD; Xiaomin Wang, MSc; Dirk Westermann, MD; Kostas Savvatis, MD; Nadine Dannemann, MSc; Carsten Skurk, MD; Denise Hilfiker-Kleiner, PhD; Toni Cathomen, PhD; Henry Fechner, DVM; Ursula Rauch, MD; Heinz-Peter Schultheiss, MD; Stephane Heymans, MD; Urs Eriksson, MD; Carmen Scheibenbogen, MD*; Wolfgang Poller, MD*

Background—CCN1 is an evolutionary ancient matricellular protein that modulates biological processes associated with tissue repair. Induction at sites of injury was observed in conditions ranging from skin wounds to cardiac diseases, including ischemic and inflammatory cardiomyopathy. Here, we provide evidence of a novel function of CCN1 as a modulator of immune cell migration.

Methods and Results—To understand the role of CCN1 in cardiomyopathies and to evaluate its therapeutic potential, we overexpressed CCN1 using an adenoviral hepatotropic vector in murine experimental autoimmune myocarditis, a model of human inflammatory cardiomyopathy. CCN1 gene transfer significantly reduced cardiac disease score and immune cell infiltration. In vivo tracking of hemagglutinin epitope–tagged CCN1 revealed binding to spleen macrophages but not to cardiomyocytes. Unexpectedly, CCN1 therapy left cardiac chemokine and cytokine expression unchanged but instead strongly inhibited the migration of spleen macrophages and lymphocytes, as evidenced by ex vivo transwell assays. In accordance with the ex vivo data, in vitro preincubation with CCN1 diminished transwell migration of human monocytes and abrogated their chemotactic response to monocyte chemoattractant protein-1, macrophage inflammatory protein-1α, and stromal cell–derived factor-1α. Further mechanistic studies showed that CCN1-driven modulation of immune cell migration is mimicked in part by cyclic RGD peptides currently in clinical evaluation for cancer therapy.

Conclusions—Our proof-of-concept study suggests investigation of CCN1 as a novel, endogenous "parent compound" for chemotaxis modulation and of cyclic RGD peptides as a class of partially CCN1-mimetic drugs with immediate potential for clinical evaluation in cardiac diseases associated with chronic pathogenic inflammation. **(*Circulation*. 2010;122:2688-2698.)**

Key Words: cardiomyopathy ■ immunomodulation ■ chemotaxis ■ migration ■ inflammation

Progressive dilation and dysfunction of heart chambers, wall thinning, and tissue fibrosis are typical of dilated cardiomyopathy, a common final pathway of heart failure that results from different causes, including monogenic defects in cardiac-expressed genes and exogenous factors such as cardiotoxic drugs or cardiotropic viruses. Inflammatory cardiomyopathy represents an important subtype of dilated cardiomyopathy and may be caused by cardiotropic virus–dependent processes or virus-triggered heart-specific autoimmunity. Cardiac expression profiling revealed that an inflammation-related gene network is strongly altered in patients with inflammatory cardiomyopathy compared with normal hearts.[1] This network includes the matricellular protein CCN1 (Cyr61), 2 other members of the CCN protein family (CTGF and WISP-1),[2,3] and the 2 CCN1-interacting proteins, thrombospondin-1 and β_1-integrin, which also mod-

Received February 11, 2010; accepted October 18, 2010.

From the Institute for Medical Immunology (M.R., C. Scheibenbogen), Charité Campus Mitte; the Department of Cardiology and Pneumology (S.K., A.E., X.W., D.W., K.S., C. Skurk, H.F., U.R., H.-P.S., W.P.), Charité Centrum 11 (Cardiovascular Medicine), Campus Benjamin Franklin; and the Institute for Virology, Campus Benjamin Franklin, Charité–Universitätsmedizin Berlin, Berlin, Germany; the Department of Cardiology, University Hospital, and Cardiovascular Research, Center for Integrative Human Physiology, University Zürich-Irehel, Zürich, Switzerland (G.K., U.E.); the Department of Cardiology (D.H.-K.) and Department of Experimental Hematology (N.D., T.C.), Hannover Medical School, Hannover, Germany; the Department of Cardiovascular Diseases and Vesalius Research Center (D.V.), Flemish Institute for Biotechnology, Catholic University Leuven, Leuven, Belgium; and the Center for Heart Failure Research (S.H.), Cardiovascular Research Institute Maastricht (CARIM), University Hospital Maastricht, Maastricht, the Netherlands.

*These authors contributed equally to this article.

The online-only Data Supplement is available with this article at http://circ.ahajournals.org/cgi/content/full/CIRCULATIONAHA.110.945261/DC1.

Correspondence to Wolfgang C. Poller, MD, Department of Cardiology and Pneumology, CBF, Charité Centrum 11 (Cardiovascular Medicine), Charité–Universitätsmedizin Berlin, Hindenburgdamm 30, D-12200 Berlin, Germany. E-mail wolfgang.poller@charite.de

Circulation **is available at http://circ.ahajournals.org** **DOI: 10.1161/CIRCULATIONAHA.110.945261**

ulate tissue repair.[4,5] To date, CCN1, a member of a gene family with 6 known members, has been characterized functionally mainly in vitro. In cell cultures, it acts in a cell type– and context-dependent manner through binding to several integrins,[6–9] including $\alpha_6\beta_1$, $\alpha_v\beta_3$, $\alpha_v\beta_5$, and $\alpha_M\beta_2$, as well as to heparan sulfate proteoglycans.[10,11] CCN1 is involved in integrin-linked kinase–mediated AKT and β-catenin–T-cell factor/Lef signaling[12] and stem cell differentiation.[13] Several lines of evidence suggest that CCN1 plays an important role in wound healing in vivo. We have previously shown that it is locally upregulated in ischemic[14] and inflammatory[1] cardiomyopathy in humans. During wound healing,[15] it coordinates a pattern of genes that promote extracellular matrix remodeling, cytokine induction, and angiogenesis, all of which are required for proper repair of tissue architecture.

Clinical Perspective on p 2698

Here, we provide for the first time evidence for a novel function of locally produced CCN1 acting as an immune signaling molecule at distant sites. To better understand the immunologic role of this novel function in the context of inflammatory heart disease and to evaluate its potential therapeutic efficacy, we used a gene-transfer approach to overexpress CCN1 in mice and assessed their susceptibility to experimental autoimmune myocarditis (EAM).[16–20] In previous studies of the EAM model, it has been shown that myosin-specific $CD4^+$ T-cell responses result in macrophage inflammatory protein-1α (MIP-1α)– and monocyte chemoattractant protein-1 (MCP-1)–driven recruitment of $CD11b^+$ monocytes to the inflamed myocardium. Blockade of MIP-1α and MCP-1 by antibodies or a dominant-negative protein significantly reduced disease severity.[21] Unexpectedly, in the present study, CCN1 overexpression reduced EAM disease scores and cardiac immune cell infiltrations without changing cardiac chemokine or chemokine receptor expression but directly inhibited the migration of circulating immune cells. CCN1 gene transfer (as used in the present proof-of-concept study), recombinant CCN1 protein, or CCN1-mimetic drugs, including cyclic RGD peptides (cRGDs), may have therapeutic potential in cardiac diseases associated with chronic pathogenic inflammation.

Methods

Cell Culture and Proteins

Peripheral blood mononuclear cells of healthy human donors (men and women 25 to 50 years old) were cultivated in Iscove's modified Dulbecco's medium supplemented with 10% AB serum. The study was reviewed and approved by the Institutional Ethics Committee, and informed consent was obtained from the patients. The proteins stromal cell–derived factor-1α (SDF-1α; R&D Systems, Minneapolis, Minn), MCP-1 (Invitrogen, San Diego, Calif), MIP-1α (Invitrogen), and CCN1 (Cell Sciences, Canton, Mass) were used at 200 ng/mL for stimulation. cRGD peptide (H4772; Bachem, Bubendorf, Switzerland) was used at 10 μmol/L for preincubation.

Development of Adenoviral CCN1 Vectors

Murine CCN1 complementary DNA (cDNA) was amplified from pAdTrack-CMV (nucleotide sequence NM_010516 [nucleotide 194-1333]) and cloned into the adenovector transfer plasmid pZS2. The recombinant plasmid was ligated to the long arm of the adenovirus strain RR5 as described previously,[22,23] and the product was transfected into HEK293 cells; a recombinant adenoviral clone, AdV-CMV-mCCN1, was amplified and purified by CsCl ultracentrifugation. For hemagglutinin epitope (HA)-tagged CCN1 vector, CCN1 cDNA was amplified from mouse muscle RNA and cloned into the pRK5 plasmid. Further cloning steps into pJet1.2 (Invitrogen) and pRK5d followed, and CCN1-HA was finally cloned into the adenovector transfer plasmid pZS2.

CCN1 Vector Evaluation in Cell Cultures

EA.hy926 cells were transduced with AdV-CMV-mCCN1, 5×10^3 particles/cell. After 72 hours, cell lysate and supernatants were collected and analyzed by Western blots under reducing conditions with an α-mouse-CCN1 primary antibody (R&D Systems) and a secondary horseradish peroxidase antibody (Dako, Glostrup, Denmark).

CCN1 Gene Transfer In Vivo

For the murine autoimmune myocarditis model, either AdV-CMV-mCCN1 or RR5, 3×10^{10} particles/mouse, was injected via tail vein into female BALB/c mice 1 week before immunization with myosin heavy chain-α (MyHC-α). AdV-CMVmCCN1-HA vector or RR5 was injected intravenously in the same doses into 10-week-old mice. For the murine myocardial infarction (MI) model, AdV-CCN1 or AdV-RR5 was also injected intravenously into male C57B/6 mice 4 days before MI induction.

Analysis of Circulating CCN1 Protein

Circulating CCN1 was studied by Western blot (see "CCN1 Vector Evaluation") of mouse sera after albumin depletion. The resulting pellet was finally resuspended with 8 mol/L urea, 2 mol/L thiourea.[24] Circulating CCN1 in heparin plasma from AdV-CCN1-HA–treated, RR5-treated, or nontreated mice was analyzed by ELISA (DGR Diagnostics, Marburg, Germany) according to the manufacturer's instructions.

Tracking of Ad-CCN1-HA In Vitro and Ex Vivo

EA.hy926 cells were transduced with 5×10^3 particles/cell of vector AdV-CMV-mCCN1-HA. Brefeldin A was added after 48 hours at 7.5 ng/mL for intracellular fluorescent-activated cell sorter (FACS) staining. After 72 hours, cells were harvested and stained with α-HA-fluorescein isothiocyanate (α-HA-FITC; Miltenyi Biotech, Bergisch Gladbach, Germany). Livers, spleens, hearts, and peripheral blood mononuclear cells generated by Ficoll gradient from AdV-CCN1-HA–transfected or nontransfected mice were taken on day 25. Single-cell suspensions were analyzed by flow cytometry with a FACS Canto II analyzer (Becton Dickinson, Franklin Lakes, NJ) and α-HA-FITC antibody or α-mouse-IgG_1 isotype control (Miltenyi Biotech). Surface staining was done for extracellular molecules CD11b, CD3e, CD11c, B220, and pan NK cells, respectively (eBioscience, San Diego, CA).

Induction of Murine Autoimmune Myocarditis

Vectors were injected intravenously 1 week before the immunization, and then female BALB/c mice were immunized with 100 μg of MyHC-α/complete Freund's adjuvant on days 0 and 7. Control mice received MyHC-α/complete Freund's adjuvant only. All analyses were performed at the peak of inflammation 21 days after immunization with MyHC-α/complete Freund's adjuvant. Myocarditis severity score was assessed on hematoxylin-and-eosin–stained sections graded 0 to 4 according to a semiquantitative score (0, no inflammatory infiltrates; 1, small foci of inflammatory cells between myocytes; 2, larger foci of 100 inflammatory cells; 3, >10% of a cross section involved; and 4, >30% of a cross section involved).

Induction and Analysis of Murine MI

MI was induced by coronary artery ligation as described previously,[25] and mice were killed 14 days later (8 animals per group). Infarction was evident from discoloration of the left ventricle. For histological analysis, hearts were fixed and sectioned (4 μm), and CD45 staining was performed to evaluate the number of leukocytes that had infiltrated the infarcted left ventricle. The number of $CD45^+$ cells in the infarcted area was counted per square millimeter, and residual

necrotic area (characterized by the presence of necrotic cells without evidence of local clearance, collagen deposition, or fibrosis) was calculated planimetrically as a percentage of the total infarct area.

RNA Analyses

Mice were injected with the vector AdV-mCCN1 or RR5 or left untreated. Mouse livers were analyzed on days 10, 20, and 40 by Northern blots and hybridized with a probe selective for recombinant mouse CCN1 (mCCN1) mRNA. For quantification versus β-actin, Scion Image Gelplot2 software (Scion Corporation, Frederick, Md) was used. Total RNA extraction and reverse-transcription reaction and real-time polymerase chain reaction were performed with mouse hearts to analyze mRNA expression levels of interferon-γ, interleukin-17A, MIP-1α, and MCP-1, respectively.

Migration Assays With Mouse Primary Cells

Single-cell suspensions were made from the spleens of RR5- or CCN1-transfected BALB/c mice. Erythrocytes were lysed with ACK buffer. Splenocytes were added to the upper well, and cells in the lower chamber were harvested after 24 hours of transmigration in an 8-μm 96-well plate (Corning, Corning, NY); stained for CD11b and CD3e, respectively; and resuspended in 100 μL of PBS plus 2% Flebogamma. A 30-μL 1:10 dilution of polystyrol beads (Comp Beads, negative control; BD, San Jose, Calif) was added to each approach. Counting was performed by FACS analysis by gating on the bead population and uptake of exactly 20 000 beads per approach. The increase was estimated as the ratio to samples without stimulation. Dead cells were estimated by a gating strategy.

Migration Assays With Human Primary Cells and THP-1 Cells

MCP-1, MIP-1α, or CCN1 was added to the lower wells of a transwell plate that contained medium plus 10% serum. Next, 1.5×10^5 peripheral blood mononuclear cells from healthy human donors purified by Ficoll gradient were suspended in culture medium plus 10% AB serum and added to the upper well for 24 hours. Cells in the lower chamber were harvested, stained with anti-CD14 antibody (BD Pharmingen), and counted as described for mouse primary cells. In preincubation experiments, cells were stimulated with CCN1 for 24 hours, then washed and restimulated as described above. Furthermore, experiments were performed with negatively magnetic-activated cell–sorted $CD3^+$ T cells and adhesion-enriched monocytes from human peripheral blood mononuclear cells. After transwell migration of THP-1, cells in the lower chamber were not harvested but were incubated with MTT (tetrazolium bromide) 5 mg/mL (Sigma, Munich, Germany) in a 1:10 dilution for 4 hour sat 37°C. Next, 0.04N HCl in isopropanol was added 1:1 into the lower well to dissolve the dark blue crystals. Plates were read at a wavelength of 570 nm against a blank without cells, and migration was calculated as the ratio to unstimulated cells. Cells were stimulated as indicated.

Western Blot Analyses

Thirty micrograms of THP-1 cell lysate was used for Western blots under denaturing and reducing conditions and transferred to a polyvinylidene fluoride membrane (Bio-Rad, Hercules, Calif). Membranes were incubated with the primary antibodies α-GAPDH (Millipore, Billerica, Mass), α-Nck2 (Abnova, Neihu District, Taipei City, Taiwan), and α-PINCH, α-ILK, AKT, and $pAKTS^{472/473}$ (BD Biosciences), as well as the secondary antibody Ig-HRP (Dako). Antibodies were incubated for 1 hour or overnight in Tris-buffered saline with Tween with 5% dry milk. For detection, a Rodeo ECL Western blot detection kit (USB Corp, Cleveland, Ohio) was used.

Chemokine Receptor Expression

Peripheral blood mononuclear cells were either left untreated or were stimulated with recombinant human CCN1 protein at 200 ng/mL for 24 hours. Cells were harvested; stained extracellularly for CCR2, CCR5, and CXCR4, respectively; and then analyzed by gating for lymphocyte and monocyte populations by FACS to compare median fluorescence intensities.

Statistical Analyses

Statistical data analyses were performed with SPSS 18.0 (SPSS Inc, Chicago, Ill). Nonparametric statistical methods were used. Continuous variables are expressed as median and interquartile range unless otherwise indicated. Univariate comparisons of 2 independent groups were performed with the Mann–Whitney *U* test. Confirmatory analyses relative to >2 groups were performed with the Kruskal-Wallis test followed by post hoc testing via Mann–Whitney *U* test with Bonferroni adjustment for multiple testing. To compare between 2 paired groups, the Wilcoxon signed rank test was applied. Because of the small sample sizes, calculations were performed with exact assumption methods (option "exact" in SPSS 18.0). A 2-tailed *P* value of $P<0.05$ was considered statistically significant. For further details, see the online-only Data Supplement.

Results

Overexpression and Tracking of Recombinant CCN1 Protein In Vivo

Multiple cell types synthesize CCN1 protein, but in contrast to common secreted proteins, CCN1 has high affinity for extracellular matrix proteins,[26] and steady state levels of endogenous CCN1 are low in the circulation. Because quantification of plasma levels[27] cannot reveal the kinetics of locally produced CCN1 in the circulation, we decided to perform in vivo tracking experiments of recombinant HA-tagged protein. For this purpose, 2 cDNAs expressing native full-length mCCN1or a variant thereof (mCCN1-HA) with a carboxy-terminal 9–amino acid HA tag (the hemagglutinin epitope YPYDVPDYA from influenza virus A) were cloned into the hepatotropic adenovirus mutant RR5 to yield the vectors AdV-mCCN1 and AdV-mCCN1-HA, respectively (Figure 1A). When AdV-mCCN1 or AdV-mCCN1-HA is expressed in EA.hy926 cells, a major fraction of CCN1 remains cell-bound, but there is free full-length CCN1 protein and an expected 21-kDa plasmin degradation product[28] in the cell supernatants (Figure 1B). By intracellular flow cytometry, recombinant CCN1 protein could be detected both intracellularly and on the surface of EA.hy926 cells (Figure 1C). In contrast to recombinant CCN1 mRNA, which carries a vector-derived bovine growth hormone (bGH) sequence at its 3′-end, endogenous CCN1 transcripts lack this sequence and therefore do not hybridize to a radioactive bGH probe as used for the Northern blot analyses shown in Figure 1D. CCN1 gene transfer by intravenous injection of vector into mice resulted in liver-specific expression of the recombinant CCN1 mRNA over several weeks (Figure 1D). Vector tropism may change owing to disease-associated processes, but Northern blot analysis of EAM and post-MI hearts did not detect vector genome within the diseased hearts. Flow cytometry revealed no binding of recombinant liver-derived HA-tagged CCN1 protein to cardiac or liver cells but did reveal strong binding to spleen and blood $CD11b^+$ cells (Figure 1E), consistent with a report demonstrating $\alpha_M\beta_2$ integrin as a CCN1 receptor on monocytes.[8] Because adenoviral gene transfer is highly liver-selective, with >99% of the vector located and expressed in this organ, the detection of HA-tagged protein on macrophages proves secretion of recombinant CCN1 protein and binding to immune cells. Furthermore, CCN1 protein could be detected by Western blot analysis in sera with 50- to 42-kDa bands corresponding to glycosylated full-length CCN1, an unglycosylated form,

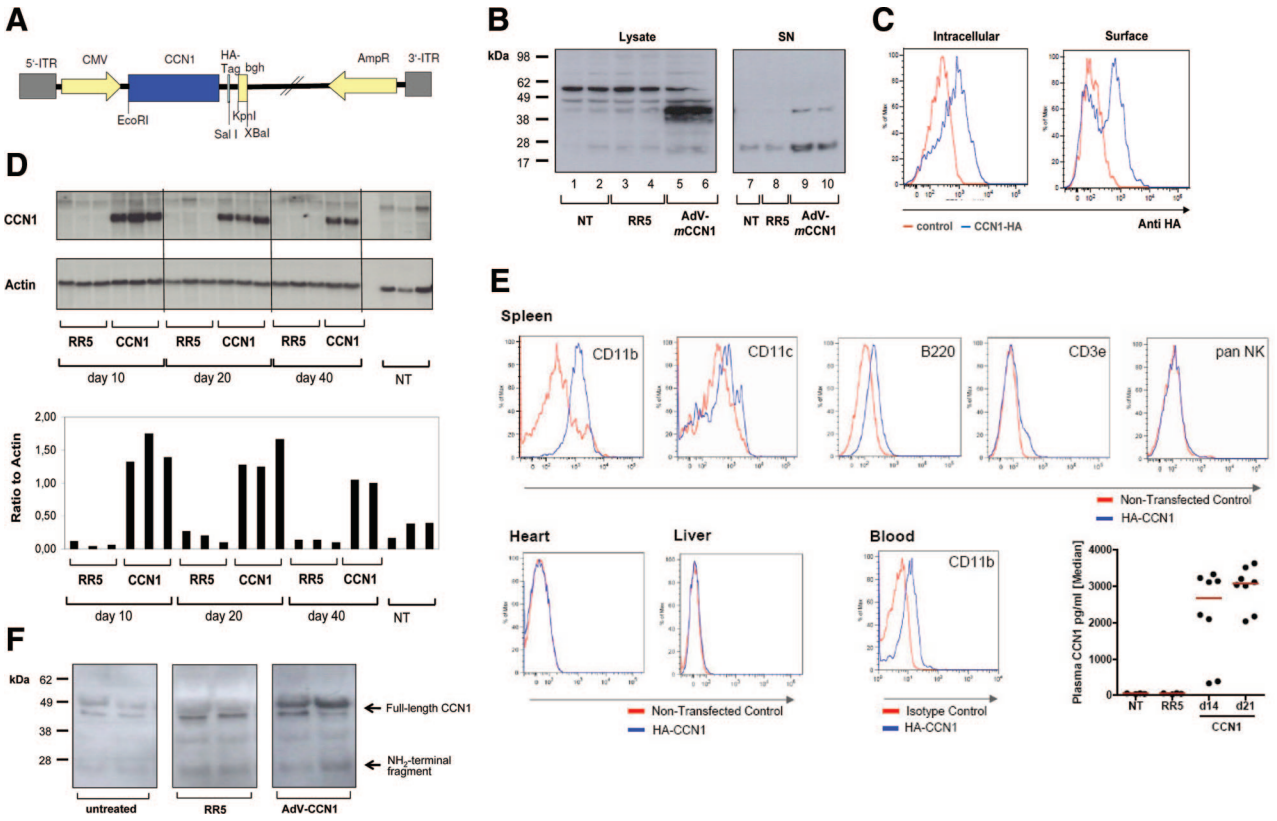

Figure 1. Overexpression and tracking of recombinant CCN1 protein in vivo. A, Recombinant adenoviral vector AdV-mCCN1 was generated by cloning of a full-length mouse CCN1 cDNA into the transfer plasmid pZS2, followed by its ligation to the long arm of adenovirus mutant RR5. AdV-mCCN1-HA expresses the 379–amino acid CCN1 linked to a carboxy-terminal 9–amino-acid hemagglutinin epitope (HA) tag (YPYDVPDYA from influenza virus A). Both vectors are under control of a cytomegalovirus (CMV) promoter and contain a bovine growth hormone termination signal (bGH), which was used in Northern blots (D) to distinguish endogenous from exogenous CCN1 mRNA. B, AdV-mCCN1–transduced EA.hy926 cells showed a 40-kDa band (representing CCN1) in the cell lysates, as shown in lanes 5/6 of the Western blot. Lysates of untreated (NT; lanes 1/2) or control vector–treated (RR5; lanes 3/4) cells showed no CCN1-specific band. In the supernatants, a full-length 40-kDa protein and a 21-kDa fragment were detected in AdV-mCCN1–transduced cells (lanes 9/10; 2 parallel samples from independent cell cultures). Lane 7 shows supernatants from a nontreated culture, and lane 8 shows supernatants from an RR5 control vector–treated cell culture. C, EA.hy926 cells transduced with AdV-mCCN1-HA were analyzed by flow cytometry to assess the distribution of the recombinant HA-tagged CCN1 protein between the intracellular compartment and the cell membrane. The red curve shows nontransfected cells, and the blue curve represents CCN-HA–transfected cells (1 of 2 independent experiments). D, Northern blot analysis of recombinant CCN1 in mouse livers shows the stability of AdV-mCCN1 expression in vivo after intravenous administration of 3×10^{10} vector particles/animal. Parallel samples from 3 nontreated animals (NT) and from AdV-CCN1–treated animals (CCN1) and mice that received control vector (RR5) are shown on days 10, 20, and 40 after vector injection (n=2 to 3). The blots were hybridized with a probe that detected the bGH termination sequence of recombinant CCN1 only (upper blot). Quantification vs β-actin is shown in the graph. E, Flow cytometric analysis of mice treated with AdV-mCCN1-HA showed no HA-tagged protein bound to the cell membrane of cardiac and hepatic cells in animals treated with CCN1-HA vector (blue curve) compared with control mice (red curve) 3 weeks after gene transfer. Membrane bound HA-tagged protein was detected in splenic and blood $CD11b^+$ cells by use of an α-HA antibody (1 of 2 independent experiments). Circulating CCN1 plasma levels (shown as median) of AdV-mCCN1-HA–treated mice (n=8) were analyzed by ELISA and compared with those of RR5-treated (n=4) and nontreated mice (n=4), respectively, on days 14 and 21 after vector injection. F, Five weeks after AdV-mCCN1 vector injection, Western blot analysis of mouse sera, after ethanol precipitation of serum albumin, showed mCCN1-specific bands that corresponded to glycosylated full-length CCN1 (≈50 kDa), an unglycosylated form at 40 kDa, and an NH_2-terminal plasmin degradation fragment at 21 kDa[28] (n=2).

and a 21-kDa plasmin degradation fragment,[28] respectively (Figure 1F). ELISA detected high CCN1-HA levels in heparin plasma from AdV-CCN1-HA–treated mice compared with RR5-treated or nontreated mice (Figure 1E). Taken together, these data show that hepatic overexpression of CCN1 vector results in a circulating CCN1 pool with binding to macrophages at distant sites.

Systemic CCN1 Therapy Attenuates EAM

To evaluate the effect of systemic CCN1 overexpression in EAM, mice were injected intravenously with CCN1 or control vector 1 week before immunization with MyHC-α, which induces EAM. As shown in Figure 2A and 2B, CCN1 treatment of mice resulted in a significant reduction of the histological disease severity scores compared with controls in hearts analyzed at the peak of cardiac inflammation 3 weeks after immunization. Because EAM leads to a strong upregulation of various cytokines and chemokines, with the monocyte-attracting chemokines MIP-1α and MCP-1[21] and interleukin-17A playing crucial roles,[20] we specifically addressed the influence of CCN1 on expression of MIP-1α and MCP-1, as well as the T-cell cytokines interleukin-17A and interferon-γ, in the diseased hearts. However, no change in the expression of these (Figure 2C) or various other chemo-

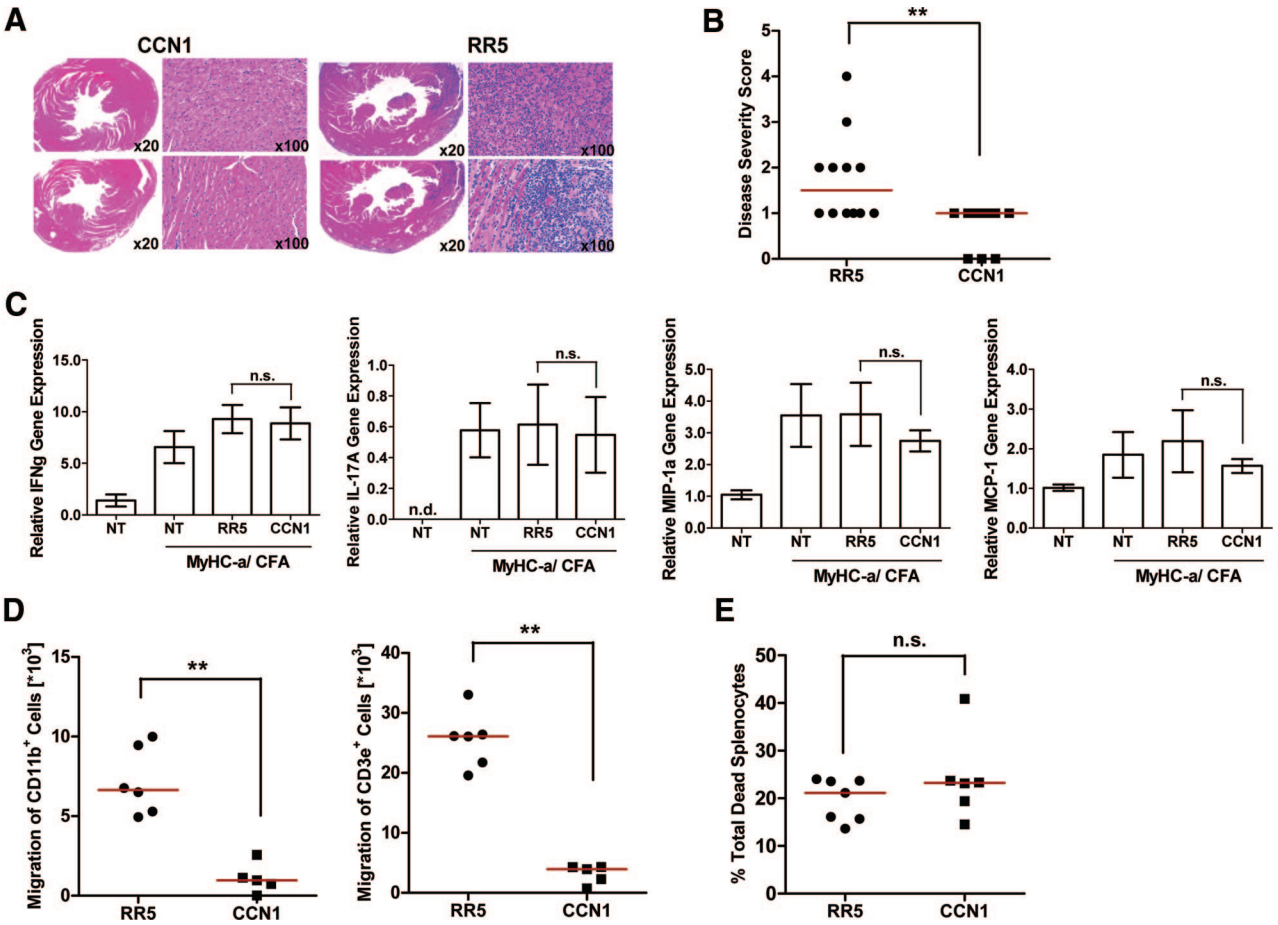

Figure 2. Systemic CCN1 therapy attenuates experimental autoimmune myocarditis. A, CCN1 or RR5 control vectors were injected intravenously 1 week before immunization of mice with a 1:1 emulsion of 100 μg/mouse MyHC-α (myosin heavy chain-α) peptide together with complete Freund adjuvant (CFA). Histological analysis by hematoxylin-and-eosin staining showed leukocyte infiltration of mouse hearts 3 weeks after the second immunization. Cardiac immune cell infiltration was greatly reduced in the hearts of mice treated with the adenoviral vector AdV-mCCN1 compared with RR5-treated mice (2 representative examples from 2 independent experiments). B, Myocarditis severity was assessed on hematoxylin-and-eosin–stained sections and graded by a semiquantitative score from 0 to 4 (0, no inflammatory infiltrates; 1, small foci of inflammatory cells between myocytes; 2, larger foci of 100 inflammatory cells; 3, >10% of a cross section involved; and 4, >30% of a cross section involved). The disease severity scores were significantly (**$P<0.01$, Mann–Whitney *U* test for independent samples) reduced by AdV-mCCN1 vector treatment (CCN1, n=10) compared with control vector–treated animals (RR5, n=12); median scores are shown. C, Real-time polymerase chain reaction analysis was performed for hearts of nontreated mice (NT), mice that had received MyHC-α/CFA alone (n=6), and mice that had received MyHC-α/CFA (n=6) with either AdV-mCCN1 (n=10) or RR5 vector (n=12). Expression of interferon-γ (IFNg), interleukin-17A (IL-17A), macrophage inflammatory protein-1α (MIP-1α), and monocyte chemoattractant protein-1 (MCP-1) was calculated as the expression level compared with Hypoxanthine-Guanine-Phosphoribosyltransferase. There was no significant reduction (shown as mean±SEM) of chemokine or cytokine expression levels in AdV-CCN1–treated mice vs RR5-treated mice. Hearts were taken at the peak of inflammation. n.s. indicates not significant (Mann–Whitney *U* test for independent samples); n.d., not detected. D, Migration assays of splenocytes isolated from mice at peak inflammation, 3 weeks after the second immunization, showed significantly (**$P<0.01$, Mann–Whitney *U* test for independent samples) reduced migration of both CD11b$^+$ macrophages (left) and CD3e$^+$ T cells (right) in AdV-CMV-CCN1–treated animals (n=6) compared with RR5-treated controls (n=6) in culture medium that contained serum after 24 hours (values shown as medians). E, Viability of splenocytes during CCN1 therapy was assessed by fluorescent-activated cell sorter gating strategy. There was no difference in absolute numbers (not shown) or frequency of dead splenocytes ex vivo after the migration assay of mice treated with CCN1 (n=6) or RR5 (n=7) vector. n.s. indicates not significant (Mann–Whitney *U* test for independent samples).

kines and chemokine receptors (data not shown) were observed. Subsequently, the migratory potential of splenic immune cells from treated animals was compared ex vivo in transwell migration assays. Remarkably, splenocytes from CCN1 vector–treated EAM mice showed strongly reduced ex vivo migration of both CD3e$^+$ T cells and CD11b$^+$ macrophages compared with controls (Figure 2D). An apoptosis-enhancing effect of CCN1 was excluded (Figure 2E).

To determine whether immune cell migration blockade as observed in EAM animals would occur only in this specific disease model, we investigated the influence of CCN1 gene transfer in MI in mice. As shown in Figure 3A and 3B, one effect common to the EAM and MI model was the suppression of cardiac immune cell infiltration. In the MI model, this suppression of cardiac inflammation was associated with diminished removal of necrotic cardiomyocytes 14 days after MI, as shown by a significantly reduced residual necrotic area in Figure 3C and 3D. No influence on cardiac fibrosis or infarct thickness was observed (data not shown). Taken together, these data imply that CCN1 therapy does not inhibit cardiac immune

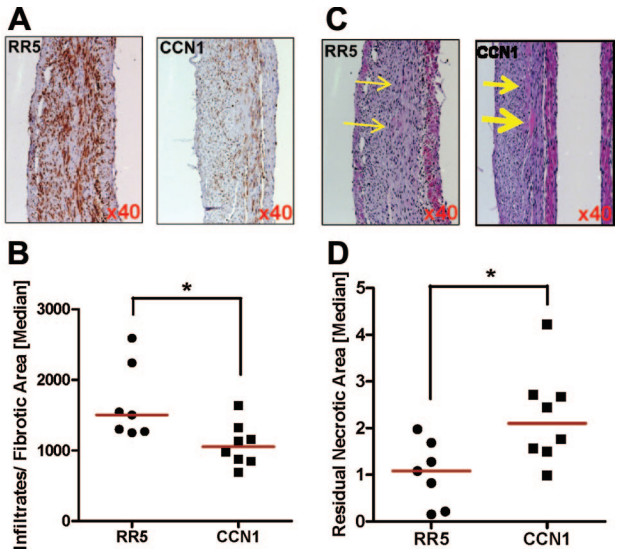

Figure 3. CCN1 attenuates cardiac inflammation after myocardial infarction. A and B, $CD45^+$ cell immunostaining of the heart on day 14 after myocardial infarction showed a significant reduction of cell infiltrates in CCN1-treated (n=7) compared with RR5-treated (n=8) mice. A shows typical examples of the $CD45^+$ immunostaining, whereas B shows the statistical evaluation for all animals, expressed as infiltrating cells per square millimeter of fibrotic area. Magnification ×40. *$P<0.05$. C and D, Histological analysis showed significantly increased areas of residual necrotic cardiomyocytes (indicated by yellow arrows) in CCN1-treated compared with RR5-treated mice. Magnification ×40. *$P<0.05$ (Mann–Whitney *U* test for independent samples). C shows typical examples of the histological analysis, whereas D shows the statistical evaluation for all animals, expressed as residual necrotic area.

cell infiltration by acting on chemokine or cytokine release within the heart but by direct inhibition of immune cell migration, and this effect on immune effector cells was the most prominent finding in 2 different disease settings.

Preincubation With CCN1 Inhibits Immune Cell Migration In Vitro

To further elucidate the mechanism of inhibition of immune cell migration by CCN1, we performed in vitro experiments on freshly isolated human immune cells. Consistent with the ex vivo data from EAM mice on CCN1 therapy, in which CCN1 serum levels were chronically elevated, in vitro preincubation with CCN1 significantly diminished the subsequent transwell migration of $CD14^+$ monocytes (Figure 4A). Although short-term exposure to CCN1 in transwell migration assays resulted in enhanced migration of human primary $CD14^+$ monocytes and $CD3^+$ lymphocytes (data not shown), significantly extending the spectrum of cells previously known to be influenced by CCN1,[6,8–10,27] in vitro preincubation with CCN1 over 24 hours completely abolished subsequent transwell migration of $CD14^+$ monocytes in response to CCN1. Of note, CCN1 preincubation left the $CD14^+$ cells refractory not only to rechallenge with CCN1 but also to chemotactic stimulation by MCP-1 and MIP-1α (Figure 4B). A similar CCN1 effect was seen for isolated negatively sorted $CD3^+$ T-cell and monocyte populations (Figure 4D). No changes in chemokine receptor expression were detected for either monocytes or lymphocytes (Figure 4E).

Similar to human primary $CD14^+$ cells, the human monocytic cell line THP-1 became refractory to chemotactic stimulation by MCP-1, MIP-1α, and SDF-1α after CCN1 preincubation (Figure 4C). As shown in Figure 4F, immunoblot quantitation of the expression levels of ILK (integrin-linked kinase), NCK2, PINCH (particularly interesting new cysteine-histidine–rich protein), and AKT, proteins involved in integrin signaling,[12,29] revealed no significant changes induced by CCN1 preincubation. mRNA expression levels of the γ-subtype of phosphoinositide 3-kinase, the target of a new class of antiinflammatory drugs,[30] and of matrix metalloproteinases 2 and 9 were likewise unchanged (data not shown). Figure I in the online-only Data Supplement compares the chemotaxis-modulating effect of CCN1 preincubation with those of drugs that block all phosphoinositide 3-kinases,[31] the phosphoinositide 3-kinase-γ subtype only,[30] AKT,[32] Rho kinase,[33] or MEK (mitogen-activated protein kinase/extracellular signal-regulated kinase kinase).[31] CCN1 preincubation blocked the effect of all chemotactic stimuli (CCN1, SDF-1α, MCP-1, and MIP-1α), whereas the spectrum of action of the small-molecule drugs was more limited.

cRGD Peptides Are Partially CCN1-Mimetic Drugs

CCN1 exerts several of its functions by binding to integrins expressed on immune cells, although various heparan sulfate proteoglycans are also involved in further cellular effects of CCN1.[10,11,34,35] Integrin targeting is currently developed for cancer therapy,[29] including the use of synthetic cRGD peptides.[36] Given their similarities with respect to integrin binding, we therefore sought to compare the effects of a cRGD peptide with those of CCN1 to further elucidate the potential role of integrins for chemotaxis modulation by CCN1, with the understanding that these synthetic compounds bind selectively to a few integrins of the α_v -type, whereas CCN1 binds to a larger spectrum of integrins and heparan sulfate proteoglycans by use of multiple and different binding sites.

Nevertheless, comparison of a cRGD peptide with CCN1 showed that preincubation with cRGD peptide also blocked migration toward CCN1, MCP-1, and SDF-1α significantly (Figure 5A). Dose-response experiments confirmed the inhibitory effect of cRGD preincubation on THP-1 cell migration over a wide dose range from 0.1 to 100 μmol/L. The inhibitory effect of cRGD peptide on the migration toward SDF-1α appeared to be less pronounced than that of CCN1 (Figure 5B). Taken together, the data suggest that integrin targeting by different agents including CCN1 and cRGD peptides may modulate immune cell chemotaxis migration, although cRGD peptides bind to fewer integrins and appear to have more limited effects than CCN1.

Discussion

CCN1 Gene Transfer Attenuates Cardiac Inflammation

In contrast to a wealth of data on the effects of CCN1 in vitro, data on its physiological functions in vivo are sparse, and its therapeutic potential against cardiovascular diseases has not yet been addressed. One limitation of in vitro studies of CCN1 stems from the fact that the functions of this protein may be profoundly altered by multiple factors not commonly

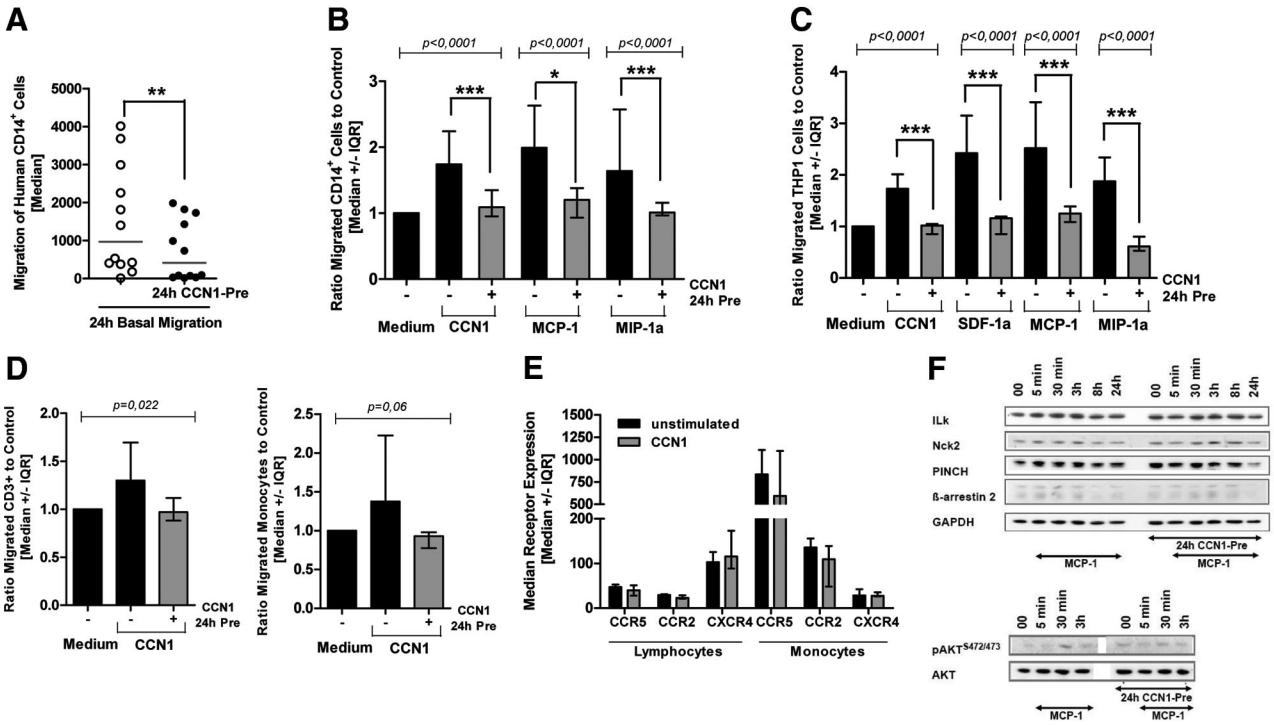

Figure 4. Preincubation with CCN1 inhibits immune cell migration in vitro. A, Basal migration (cell numbers) of freshly isolated human CD14$^+$ cells (n=12) was significantly (**$P<0.01$, Wilcoxon signed rank test for dependent samples) reduced during migration in culture medium that contained 10% serum for cells that were preincubated with CCN1 at 200 ng/mL for 24 hours compared with CD14$^+$ cells from the same donor that were not preincubated. B, Prolonged CCN1 exposure (+CCN1 24h Pre) resulted in abrogation of the chemotaxis-stimulating effects of CCN1 itself and of the chemokines monocyte chemoattractant protein-1 (MCP-1) and macrophage inflammatory protein-1α (MIP-1α; black bars). After 24 hours of preincubation with 200 ng/mL CCN1, the chemokines were no longer able to stimulate monocyte chemotaxis (gray bars). n=9. *P* values on top indicate Kruskal-Wallis test results for the 3 experimental groups (for chemokines CCN1, MCP-1, and MIP-1α), each comprising cells with or without preincubation or with medium control. Asterisks indicate significant effects of preincubation at the corrected significance level $\alpha_{corr}=0.0167$, with $P_{corr}<0.05$ (*) and $P_{corr}<0.001$ (***), respectively, according to the Mann–Whitney *U* test for independent samples with Bonferroni adjustment for multiple testing. Compare this in vitro finding with the ex vivo data shown in Figure 2D. C, Similar to the situation with primary human monocytes, monocytic THP-1 cells were stimulated with 200 ng/mL CCN1, SDF-1α), MCP-1, and MIP-1α for 24 hours with (gray bars) and without (black bars) 24-hour 200-ng/mL CCN1 preincubation (CCN1 24h Pre). n=9/10. *P* values on top indicate Kruskal-Wallis test results for the 4 experimental groups (for chemokines CCN1, SDF-1α, MCP-1, MIP-1α), each comprising cells with or without preincubation or with medium control. Asterisks indicate significant effects of preincubation on the corrected significance level $\alpha_{corr}=0.0167$, with $P_{corr}<0.001$ (***) according to Mann–Whitney *U* test for independent samples with Bonferroni adjustment for multiple testing. D, Migration experiments were performed with negatively magnetic-activated cell–sorted CD3$^+$ T cells (untouched; left) and adhesion-enriched monocytes (right) from human peripheral blood mononuclear cells. n=4 donors. *P* values on top of the left and right panels indicate Kruskal-Wallis test results for the 2 experimental groups (sorted CD3$^+$ T cells, adhesion-enriched monocytes), each comprising cells with or without preincubation or with medium control. CCN1 stimulation itself led to enhanced migration of both CD3$^+$ T cells and monocytes (black bars), but CCN1 preincubation for 24 hours (CCN1 24h Pre) led to impaired migration (gray bars). E, Median fluorescence intensities in peripheral blood mononuclear cells were measured to quantify extracellular expression of chemokine receptors CCR2, CCR5, and CXCR4 after 24 hours of CCN1 stimulation at 200 ng/mL and compared with unstimulated cells from the same donor by extracellular staining (n=6; Mann–Whitney *U* test for independent samples). F, Intracellular signal transduction proteins linked to integrins and AKT phosphorylation were analyzed by Western blot analysis. Left side of each blot shows protein expression levels of integrin-linked kinase (ILK), Nck2, PINCH (particularly interesting new cysteine-histidine–rich protein), and β-arrestin 2, which blocks G-protein–mediated signaling, at various time points (5 minutes, 30 minutes, 3 hours, 8 hours, and 24 hours) after addition of MCP-1 200 ng/mL. Blots on the right side show the same analyses but with addition of MCP-1 after a preceding preincubation with CCN1 at 200 ng/mL for 24 hours (1 of at least 2 independent experiments). Densitometric analysis (online-only Data Supplement Figure II) showed, as expected, that MCP-1 induced upregulation of ILK, β-arrestin, PINCH, and pAKTS$^{472/473}$, but it detected no inhibitory effect of 24-hour CCN1 preincubation on these inductions. IQR indicates interquartile range.

present in vitro. These include numerous interacting proteins, homodimerization via CT domains, and multimer formations via VWC domains.[34,35] Although isolated functions of the 4 CCN domains have been clarified to a considerable degree at the molecular and cellular level, the complexity of their known molecular interactions makes it impossible to predict their overall effect in the intact organism. A CCN1 knockout model has provided important data on functions during development,[37] but for the adult organism, CCN1 protein tracking and modulation in disease models is likely to contribute to a more comprehensive picture of its functions.

Using this approach, we obtained direct evidence of a novel in vivo function of CCN1 acting as an inhibitor of immune cell chemotaxis and migration. In an initial series of experiments, tracking of recombinant CCN1 protein in vivo showed that hepatic CCN1 overexpression resulted in a circulating CCN1 pool that bound to splenic macrophages and blood monocytes. In a second set of experiments, we

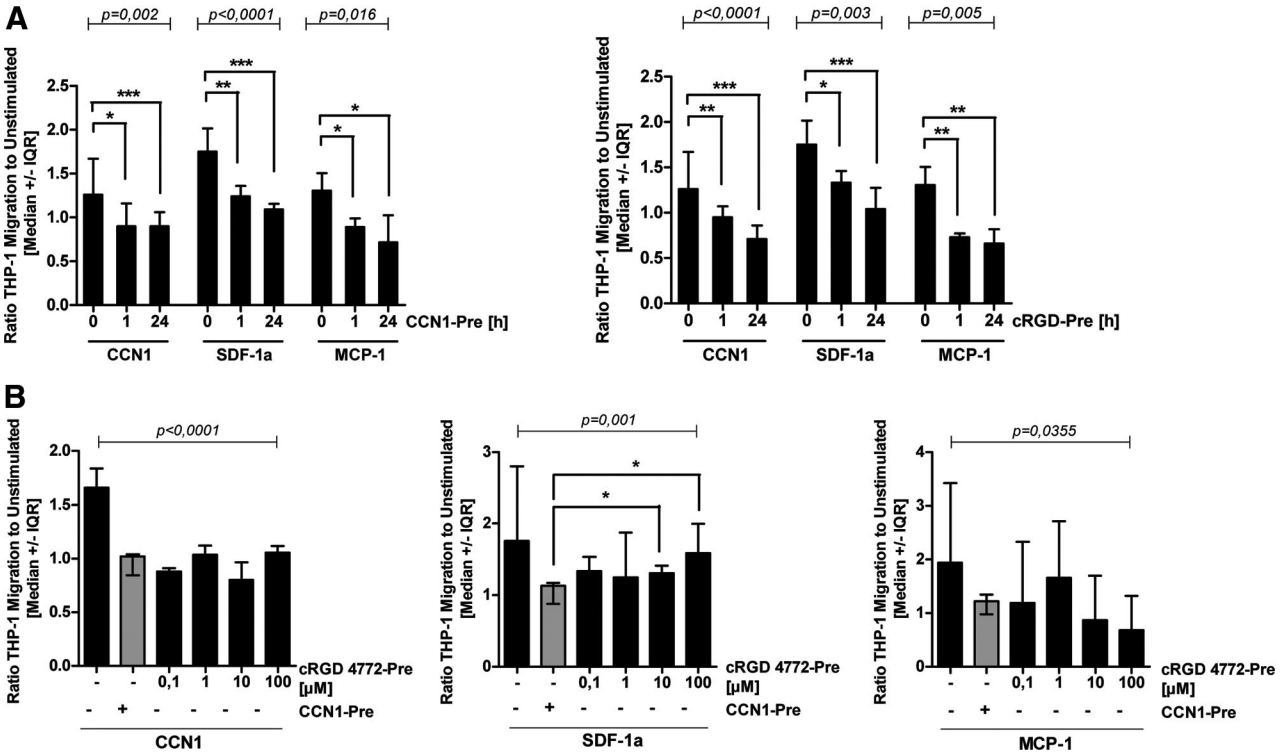

Figure 5. cRGD peptides are partially CCN1-mimetic drugs. A, CCN1, SDF-1α), and MCP-1 at 200 ng/mL are chemotactic for monocytic THP-1 cells. Graph on the left shows the influence of CCN1 preincubation and graph on the right shows the influence of cRGD preincubation on these chemotactic processes. Preincubation for 1 hour or 24 hours with 200 ng/mL CCN1 (CCN1-Pre; left) or cRGD (cRGD-Pre; right) resulted in significant abrogation of the chemotaxis-stimulating effects of CCN1, SDF-1α, and MCP-1 compared with reference cells without preincubation (left bars in each triplet, designated "0"). All comparisons are based on separate cell samples obtained at baseline. Two of the samples (1 hour, 24 hours) were preincubated with 200 ng/mL CCN1 (left graph) and another 2 with 10 μmol/L cRGD (right graph). Neither CCN1 nor cRGD was added to the reference. For each preincubated group (CCN1 and cRGD, respectively), 1 of the cell samples was analyzed after 1 hour and the other after 24 hours. Comparable results were obtained for 1 hour or 24 hours of preincubation with CCN1 protein or cRGD peptide (n=9 to 12). *P* values on top of each triplet indicate Kruskal-Wallis test results for the 6 experimental groups (for chemokines CCN1, SDF-1α, MCP-1), each comprising cells without preincubation or with preincubation for 1 hour or 24 hours. Asterisks indicate significant effects of preincubation on the corrected significance level α_{corr}=0.0167, with P_{corr}<0.05 (*), P<0.01 (**), and P_{corr}<0.001 (***), respectively, according to Mann–Whitney *U* test for independent samples with Bonferroni adjustment for multiple testing. B, Dose dependency of cRGD preincubation is shown for 0.1, 1.0, 10, and 100 μmol/L cRGD peptide on THP-1 cells stimulated with 200 ng/mL CCN1, SDF-1α, and MCP-1, respectively. The migration-promoting effect of all 3 chemokines was inhibited over a broad dose range of cRGD. Inhibition of SDF-1α–induced migration by cRGD preincubation appears to be less pronounced than that by preincubation with CCN1 under these in vitro conditions (gray bars). n=6/9. *P* value on top of the SDF-1α graph indicates Kruskal-Wallis test result for the 6 experimental groups shown. Asterisk in the SDF-1α graph indicates a difference on the corrected significance level α_{corr}=0.001, with P_{corr}<0.05 according to Mann–Whitney *U* test with Bonferroni adjustment for multiple testing. IQR indicates interquartile range.

found that chronic overexpression of CCN1 ameliorated the course of EAM, a local autoimmune-triggered inflammation associated with severe cardiac injury. Unexpectedly, CCN1 gene therapy did not modulate cardiac expression of the chemokines MCP-1 and MIP-1α or of interleukin-17A, which are known to be key mediators of EAM.[20,21] Instead, direct ex vivo analysis of circulating immune cells from mice during CCN1 gene therapy revealed that their migratory capacity ex vivo was greatly reduced. Although inhibition of migration of vascular smooth muscle cells by CCN5 has been described,[38] CCN1 has so far been solely considered as a protein that stimulates cell migration. In accordance with its described effect on fibroblasts[6] and $CD34^+$ stem cells,[27] we observed that CCN1 has an early migration-supporting effect on monocytes. Preincubation with CCN1, however, completely abrogated not only the migration-stimulating effect of CCN1 but also the chemotactic response to MCP-1, MIP-1α, and SDF-1α. Of interest, CCN1 suppressed cardiac immune cell infiltration strongly, both in the autoimmune and the MI model, consistent with the assumption of direct blockade of circulating monocytes by CCN1. Such a mechanism of action, also supported by the in vitro transwell data, would be essentially independent of specific local processes (eg, chemokine/cytokine patterns), which vary depending on the type of injury (ischemic, autoimmune, viral, or gene defect). Beyond the present study's delineation of CCN1 as a novel immune cell migration modulator, differential effects of CCN1 dose and timing with respect to disease course need to be evaluated further in the future. We also currently do not know whether there are different effects of CCN1 on the migration of immune cell subpopulations in vivo. In the transwell assays, cell proliferation did not influence the results, but in vivo, T cells may proliferate locally in the heart after immigration in response to antigen, whereas monocytes do not. This, along with the fact that the overwhelming fraction of heart-infiltrating cells in EAM are monocytes, may explain the

unchanged cardiac expression of the T-cell cytokines interleukin-17 and interferon-γ despite reduce immune cell infiltration.

CCN1 Action on Immune Cells Is Mimicked in Part by cRGD Peptides

Importantly, the in vitro transwell migration experiments as conducted do not involve any immune cell–endothelium interactions but reflect direct effects of CCN1 on the immune cells themselves. Clearly, under such in vitro conditions, it is the direct interaction of CCN1 with 1 or more of the known receptors on the immune cells that results in their "reprogramming" by prolonged exposure. This must be assumed to occur also in vivo during CCN1 therapy. Given the fact that CCN1 is an evolutionary highly conserved endogenous protein, the biphasic profile is likely to confer important homeostatic functions, including an optimized response of inflammatory effector cells to tissue injury. It is tempting to speculate as to whether CCN1 can also result in systemic depression of migration under pathophysiological conditions, but that question is beyond the scope of this therapy-directed report and requires additional studies. Likewise beyond its scope is a full elucidation of the mechanism by which CCN1 modulates immune cell migration at the molecular and cellular level. Global Western blot analyses (Figure 4D) were unable to detect intracellular polarization processes[39,40] known to determine the dynamic transitions between immobile state, random migration, and directed migration (chemotaxis, haptotaxis) of immune cells. Instead, life-cell microscopy will be required for a detailed description of CCN1 and cRGD peptide effects on these processes. Nevertheless, the present data already indicate that both random migration (Figures 2D and 4A) and directed migration along a chemotactic gradient (Figures 4B, 4C, and 5) are affected by these agents. At the systemic level, it will be interesting to determine whether CCN1 treatment influences the generation of T-cell responses and the ability of antigen-presenting cells to migrate to draining lymph nodes.

Because CCN1 is known to exert part of its function by binding to various integrins, we sought to compare its effect on immune cell migration with that of the integrin-binding cRGD peptides currently developed as antiangiogenic and antiproliferative agents for cancer therapy.[29,36] With respect to our comparison of cRGD peptides with CCN1 (Figure 5B), it is of interest that these synthetic compounds bind selectively to one type of integrins only, whereas the complex, 4-domain protein CCN1 binds to a broad spectrum of integrins, including $\alpha_6\beta_1$, $\alpha_v\beta_3$, $\alpha_v\beta_5$, and $\alpha_M\beta_2$, and to heparan sulfate proteoglycans.[41] Remarkably, direct comparison of CCN1 with an integrin-interacting cRGD peptide nevertheless showed a similar migration-inhibiting effect, although chemotaxis toward SDF-1α was not blocked as efficiently as with CCN1. Thus, the present studies describe a novel migration-inhibiting effect for cRGD peptides, which may be of considerable relevance for both anticancer and antiinflammatory treatment. Chronic CCN1 exposure modifies the immune cell response to a broad spectrum of chemotactic stimuli in vitro and in vivo, in contrast to specific chemokine or chemokine receptor–blocking agents[21] with their known limitations[42] that arise from the fact that in most inflammatory diseases, multiple chemokines and chemokine receptors are involved, and no single target of outstanding pathogenetic importance exists. Although the chemokine target spectrum of CCN1 appears to be broader, evaluation of cRGD peptides for immunomodulation and the treatment of inflammatory diseases appears warranted on the basis of these data.

Possible Implications for the Treatment of Cardiac Diseases

Different antiinflammatory therapeutic strategies are required for distinct target diseases,[43] and CCN1 may expand the spectrum of tools for chemotaxis modulation and offer new therapeutic perspectives for important cardiac[44–46] and autoimmune[30,47] disorders. Therapeutic interest in CCN1 was initially triggered by a genomics study in humans,[1] which resembles the path of other investigations that have used genomic approaches to drive novel compound pipelines.[48] Before any antiinflammatory approach is undertaken, it will be crucial to delineate the distinction between acute inflammation that supports tissue repair and regeneration versus chronic inflammation without reparative advantage but that induces progressive tissue injury. With respect to the latter type of inflammation, further investigation of CCN1 as a new parent compound for immune cell migration modulation appears warranted, as well as of cRGD peptides as a first class of partially CCN1-mimetic drugs with immediate potential for clinical evaluation in cardiac disorders associated with chronic pathogenic inflammation (eg, autoimmune heart disease and cardiac transplant rejection).

Acknowledgments

The authors thank Andrea Stroux, MSc, Department for Biometry and Clinical Epidemiology, Charité–Universitätsmedizin Berlin, for expert statistical advice; Dr M. Herkert of DRG Instruments, Marburg, Germany, who generously provided the anti-CCN1 ELISA; and Sandra Bauer for excellent technical assistance.

Sources of Funding

This work has been supported by Deutsche Forschungsgemeinschaft through research network SFB Transregio 19 (by grant C5 to Dr Poller, Dr Scheibenbogen, and Dr Cathomen; grant A2 to Drs Westermann and Schultheiss). Dr Eriksson is the recipient of a Swiss National Foundation professorship and received support from the Swiss Life Foundation, Olga Maenfisch Foundation, and Swiss Heart Foundation. This work was further supported by an Ingenious Hypercare Network of Excellence European Union grant and a Dutch Scientific Organization VIDI grant to Dr Heymans. Dr Vanhoutte is supported by a postdoctoral fellowship of the Research Foundation Flanders (FWO, Belgium). M. Rother is supported by Berlin-Brandenburg School for Regenerative Therapies, Deutsche Forschungsgemeinschaft Graduate School 203.

Disclosures

None.

References

1. Wittchen F, Suckau L, Witt H, Skurk C, Lassner D, Fechner H, Sipo I, Ungethum U, Ruiz P, Pauschinger M, Tschope C, Rauch U, Kuhl U, Schultheiss HP, Poller W. Genomic expression profiling of human inflammatory cardiomyopathy (DCMi) suggests novel therapeutic targets. *J Mol Med*. 2007;85:257–271.
2. Chaqour B, Goppelt-Struebe M. Mechanical regulation of the Cyr61/CCN1 and CTGF/CCN2 proteins. *FEBS J*. 2006;273:3639–3649.

3. Colston JT, de la Rosa SD, Koehler M, Gonzales K, Mestril R, Freeman GL, Bailey SR, Chandrasekar B. Wnt-induced secreted protein-1 is a prohypertrophic and profibrotic growth factor. *Am J Physiol Heart Circ Physiol*. 2007;293:H1839–H1846.
4. Frangogiannis NG, Ren G, Dewald O, Zymek P, Haudek S, Koerting A, Winkelmann K, Michael LH, Lawler J, Entman ML. Critical role of endogenous thrombospondin-1 in preventing expansion of healing myocardial infarcts. *Circulation*. 2005;111:2935–2942.
5. Krishnamurthy P, Subramanian V, Singh M, Singh K. β_1 Integrins modulate β-adrenergic receptor-stimulated cardiac myocyte apoptosis and myocardial remodeling. *Hypertension*. 2007;49:865–872.
6. Grzeszkiewicz TM, Kirschling DJ, Chen N, Lau LF. CYR61 stimulates human skin fibroblast migration through integrin $\alpha_V\beta_5$ and enhances mitogenesis through integrin $\alpha_v\beta_3$, independent of its carboxyl-terminal domain. *J Biol Chem*. 2001;276:21943–21950.
7. Schober JM, Lau LF, Ugarova TP, Lam SC. Identification of a novel integrin $\alpha_M\beta_2$ binding site in CCN1 (CYR61), a matricellular protein expressed in healing wounds and atherosclerotic lesions. *J Biol Chem*. 2003;278:25808–25815.
8. Schober JM, Chen N, Grzeszkiewicz TM, Jovanovic I, Emeson EE, Ugarova TP, Ye RD, Lau LF, Lam SC. Identification of integrin $\alpha_M\beta_2$ as an adhesion receptor on peripheral blood monocytes for Cyr61 (CCN1) and connective tissue growth factor (CCN2): immediate-early gene products expressed in atherosclerotic lesions. *Blood*. 2002;99:4457–4465.
9. Chen N, Leu SJ, Todorovic V, Lam SC, Lau LF. Identification of a novel integrin $\alpha_V\beta_3$ binding site in CCN1 (CYR61) critical for pro-angiogenic activities in vascular endothelial cells. *J Biol Chem*. 2004;279:44166–44176.
10. Grzeszkiewicz TM, Lindner V, Chen N, Lam SC, Lau LF. The angiogenic factor cysteine-rich 61 (CYR61, *CCN1*) supports vascular smooth muscle cell adhesion and stimulates chemotaxis through integrin $\alpha_6\beta_1$ and cell surface heparan sulfate proteoglycans. *Endocrinology*. 2002;143:1441–1450.
11. Leu SJ, Chen N, Chen CC, Todorovic V, Bai T, Juric V, Liu Y, Yan G, Lam SC, Lau LF. Targeted mutagenesis of the angiogenic protein CCN1 (CYR61). Selective inactivation of integrin $\alpha_6\beta_1$-heparan sulfate proteoglycan coreceptor-mediated cellular functions. *J Biol Chem*. 2004;279:44177–44187.
12. Xie D, Yin D, Tong X, O'Kelly J, Mori A, Miller C, Black K, Gui D, Said JW, Koeffler HP. Cyr61 is overexpressed in gliomas and involved in integrin-linked kinase-mediated Akt and β-catenin-TCF/Lef signaling pathways. *Cancer Res*. 2004;64:1987–1996.
13. Si W, Kang Q, Luu HH, Park JK, Luo Q, Song WX, Jiang W, Luo X, Li X, Yin H, Montag AG, Haydon RC, He TC. CCN1/Cyr61 is regulated by the canonical Wnt signal and plays an important role in Wnt3A-induced osteoblast differentiation of mesenchymal stem cells. *Mol Cell Biol*. 2006;26:2955–2964.
14. Hilfiker-Kleiner D, Kaminski K, Kaminska A, Fuchs M, Klein G, Podewski E, Grote K, Kiian I, Wollert KC, Hilfiker A, Drexler H. Regulation of proangiogenic factor CCN1 in cardiac muscle: impact of ischemia, pressure overload, and neurohumoral activation. *Circulation*. 2004;109:2227–2233.
15. Chen CC, Mo FE, Lau LF. The angiogenic factor Cyr61 activates a genetic program for wound healing in human skin fibroblasts. *J Biol Chem*. 2001;276:47329–47337.
16. Valaperti A, Marty RR, Kania G, Germano D, Mauermann N, Dirnhofer S, Leimenstoll B, Blyszczuk P, Dong C, Mueller C, Hunziker L, Eriksson U. $CD11b^+$ monocytes abrogate Th17 CD4+ T cell-mediated experimental autoimmune myocarditis. *J Immunol*. 2008;180:2686–2695.
17. Kania G, Blyszczuk P, Valaperti A, Dieterle T, Leimenstoll B, Dirnhofer S, Zulewski H, Eriksson U. Prominin-1^+/$CD133^+$ bone marrow-derived heart-resident cells suppress experimental autoimmune myocarditis. *Cardiovasc Res*. 2008;80:236–245.
18. Marty RR, Dirnhofer S, Mauermann N, Schweikert S, Akira S, Hunziker L, Penninger JM, Eriksson U. MyD88 signaling controls autoimmune myocarditis induction. *Circulation*. 2006;113:258–265.
19. Rangachari M, Mauermann N, Marty RR, Dirnhofer S, Kurrer MO, Komnenovic V, Penninger JM, Eriksson U. T-bet negatively regulates autoimmune myocarditis by suppressing local production of interleukin 17. *J Exp Med*. 2006;203:2009–2019.
20. Eriksson U, Ricci R, Hunziker L, Kurrer MO, Oudit GY, Watts TH, Sonderegger I, Bachmaier K, Kopf M, Penninger JM. Dendritic cell-induced autoimmune heart failure requires cooperation between adaptive and innate immunity. *Nat Med*. 2003;9:1484–1490.
21. Goser S, Ottl R, Brodner A, Dengler TJ, Torzewski J, Egashira K, Rose NR, Katus HA, Kaya Z. Critical role for monocyte chemoattractant protein-1 and macrophage inflammatory protein-1alpha in induction of experimental autoimmune myocarditis and effective anti-monocyte chemoattractant protein-1 gene therapy. *Circulation*. 2005;112:3400–3407.
22. Suckau L, Fechner H, Chemaly E, Krohn S, Hadri L, Kockskämper J, Westermann D, Bisping E, Ly H, Wang X, Kawase Y, Chen J, Liang L, Sipo I, Vetter R, Weger S, Kurreck J, Erdmann V, Tschope C, Pieske B, Lebeche D, Schultheiss H, Hajjar R, Poller W. Chronic cardiac-targeted RNA interference for the treatment of heart failure restores cardiac function and reduces pathological hypertrophy. *Circulation*. 2009;119:1241–1252.
23. Fechner H, Noutsias M, Tschoepe C, Hinze K, Wang X, Escher F, Pauschinger M, Dekkers D, Vetter R, Paul M, Lamers J, Schultheiss HP, Poller W. Induction of coxsackievirus-adenovirus-receptor expression during myocardial tissue formation and remodeling: identification of a cell-to-cell contact-dependent regulatory mechanism. *Circulation*. 2003;107:876–882.
24. Colantonio DA, Dunkinson C, Bovenkamp DE, Van Eyk JE. Effective removal of albumin from serum. *Proteomics*. 2005;5:3831–3835.
25. Schellings MW, Vanhoutte D, Swinnen M, Cleutjens JP, Debets J, van Leeuwen RE, d'Hooge J, Van de Werf F, Carmeliet P, Pinto YM, Sage EH, Heymans S. Absence of SPARC results in increased cardiac rupture and dysfunction after acute myocardial infarction. *J Exp Med*. 2009;206:113–123.
26. Kireeva ML, Latinkic BV, Kolesnikova TV, Chen CC, Yang GP, Abler AS, Lau LF. Cyr61 and Fisp12 are both ECM-associated signaling molecules: activities, metabolism, and localization during development. *Exp Cell Res*. 1997;233:63–77.
27. Grote K, Salguero G, Ballmaier M, Dangers M, Drexler H, Schieffer B. The angiogenic factor CCN1 promotes adhesion and migration of circulating $CD34^+$ progenitor cells: potential role in angiogenesis and endothelial regeneration. *Blood*. 2007;110:877–885.
28. Pendurthi UR, Tran TT, Post M, Rao LV. Proteolysis of CCN1 by plasmin: functional implications. *Cancer Res*. 2005;65:9705–9711.
29. Hehlgans S, Haase M, Cordes N. Signalling *via* integrins: implications for cell survival and anticancer strategies. *Biochim Biophys Acta*. 2007;1775:163–180.
30. Camps M, Ruckle T, Ji H, Ardissone V, Rintelen F, Shaw J, Ferrandi C, Chabert C, Gillieron C, Francon B, Martin T, Gretener D, Perrin D, Leroy D, Vitte PA, Hirsch E, Wymann MP, Cirillo R, Schwarz MK, Rommel C. Blockade of PI3K-γ suppresses joint inflammation and damage in mouse models of rheumatoid arthritis. *Nat Med*. 2005;11:936–943.
31. Arefieva TI, Kukhtina NB, Antonova OA, Krasnikova TL. MCP-1-stimulated chemotaxis of monocytic and endothelial cells is dependent on activation of different signaling cascades. *Cytokine*. 2005;31:439–446.
32. Dieterle A, Orth R, Daubrawa M, Grotemeier A, Alers S, Ullrich S, Lammers R, Wesselborg S, Stork B. The Akt inhibitor triciribine sensitizes prostate carcinoma cells to TRAIL-induced apoptosis. *Int J Cancer*. 2009;125:932–941.
33. Menschikowski M, Hagelgans A, Heyne B, Hempel U, Neumeister V, Goez P, Jaross W, Siegert G. Statins potentiate the IFN-γ-induced upregulation of group IIA phospholipase A2 in human aortic smooth muscle cells and HepG2 hepatoma cells. *Biochim Biophys Acta*. 2005;1733:157–171.
34. Holbourn KP, Acharya KR, Perbal B. The CCN family of proteins: structure-function relationships. *Trends Biochem Sci*. 2008;33:461–473.
35. Desnoyers L. Structural basis and therapeutic implication of the interaction of CCN proteins with glycoconjugates. *Curr Pharm Des*. 2004;10:3913–3928.
36. Reynolds AR, Hart IR, Watson AR, Welti JC, Silva RG, Robinson SD, Da Violante G, Gourlaouen M, Salih M, Jones MC, Jones DT, Saunders G, Kostourou V, Perron-Sierra F, Norman JC, Tucker GC, Hodivala-Dilke KM. Stimulation of tumor growth and angiogenesis by low concentrations of RGD-mimetic integrin inhibitors. *Nat Med*. 2009;15:392–400.
37. Mo FE, Muntean AG, Chen CC, Stolz DB, Watkins SC, Lau LF. CYR61 (CCN1) is essential for placental development and vascular integrity. *Mol Cell Biol*. 2002;22:8709–8720.
38. Lake AC, Bialik A, Walsh K, Castellot JJ Jr. CCN5 is a growth arrest-specific gene that regulates smooth muscle cell proliferation and motility. *Am J Pathol*. 2003;162:219–231.
39. Friedl P, Weigelin B. Interstitial leukocyte migration and immune function. *Nat Immunol*. 2008;9:960–969.

40. Wong CH, Heit B, Kubes P. Molecular regulators of leucocyte chemotaxis during inflammation. *Cardiovasc Res*. 2010;86:183–191.
41. Bishop JR, Schuksz M, Esko JD. Heparan sulphate proteoglycans fine-tune mammalian physiology. *Nature*. 2007;446:1030–1037.
42. Horuk R. Chemokine receptor antagonists: overcoming developmental hurdles. *Nat Rev Drug Discov*. 2009;8:23–33.
43. Mackay CR. Moving targets: cell migration inhibitors as new anti-inflammatory therapies. *Nat Immunol*. 2008;9:988–998.
44. Morimoto H, Takahashi M, Izawa A, Ise H, Hongo M, Kolattukudy PE, Ikeda U. Cardiac overexpression of monocyte chemoattractant protein-1 in transgenic mice prevents cardiac dysfunction and remodeling after myocardial infarction. *Circ Res*. 2006;99:891–899.
45. Dewald O, Zymek P, Winkelmann K, Koerting A, Ren G, Abou-Khamis T, Michael LH, Rollins BJ, Entman ML, Frangogiannis NG. CCL2/monocyte chemoattractant protein-1 regulates inflammatory responses critical to healing myocardial infarcts. *Circ Res*. 2005;96:881–889.
46. Frangogiannis NG, Dewald O, Xia Y, Ren G, Haudek S, Leucker T, Kraemer D, Taffet G, Rollins BJ, Entman ML. Critical role of monocyte chemoattractant protein-1/CC chemokine ligand 2 in the pathogenesis of ischemic cardiomyopathy. *Circulation*. 2007;115:584–592.
47. Barber DF, Bartolome A, Hernandez C, Flores JM, Redondo C, Fernandez-Arias C, Camps M, Ruckle T, Schwarz MK, Rodriguez S, Martinez AC, Balomenos D, Rommel C, Carrera AC. PI3K-γ inhibition blocks glomerulonephritis and extends lifespan in a mouse model of systemic lupus. *Nat Med*. 2005;11:933–935.
48. Plump AS, Lum PY. Genomics and cardiovascular drug development. *J Am Coll Cardiol*. 2009;53:1089–1100.

CLINICAL PERSPECTIVE

CCN1 is an evolutionary ancient matricellular protein that modulates biological processes associated with tissue repair. Here, we provide evidence of a novel function of CCN1 as a modulator of immune cell migration, with therapeutic potential in diseases associated with chronic pathogenic inflammation. In the current proof-of-concept study, we used CCN1 gene transfer to evaluate its therapeutic potential in animal models of human inflammatory cardiomyopathy and myocardial infarction. CCN1 therapy significantly reduced immune cell infiltration in both models. CCN1 exposure resulted in strongly suppressed migration of immune cells both in vivo and in vitro and abrogated their chemotactic response to various chemokines. These data suggest that CCN1 has potential as a new broad-spectrum immune cell migration inhibitor, in contrast to specific chemokine- or chemokine receptor–blocking agents with their known limitations arising from the fact that in most inflammatory diseases, multiple chemokines and chemokine receptors are involved and no single target of outstanding pathogenic importance exists. From a clinical translational perspective, it is of interest that the effects of the endogenous protein CCN1 on immune cell chemotaxis and migration are partially mimicked by cyclic RGD peptides that are currently being evaluated in clinical trials, although as yet for cancer therapy only. Our proof-of-concept study suggests further investigation of CCN1 as a new parent compound for immune cell migration modulation and of cyclic RGD peptides as CCN1 mimetics with immediate potential for clinical evaluation in cardiac diseases associated with chronic pathogenic inflammation.

SUPPLEMENTAL MATERIAL

for the Manuscript by Rother *et al.*

The Matricellular Signaling Molecule CCN1 Attenuates Experimental Autoimmune Myocarditis by Acting as a Novel Immune Cell Migration Modulator

SUPPLEMENTAL METHODS

Cell Cultures and Proteins

Eahy.926 cells were cultured in DMEM (Dulbecco's Modified Eagle) medium with Glutamax-I (Invitrogen, San Diego, CA USA), 10% fetal calf serum (FCS) and 1x HAT. Mouse splenocytes were cultured in RPMI 1640 supplemented with 5% FCS, THP1 with 10% FCS. Peripheral blood mononuclear cells (PBMCs) of healthy human donors (male and female aged 25 to 50) were cultivated in IMDM (Iscove's Modified Dulbecco's Medium) supplemented with 10% AB serum. The study was reviewed and approved by the Institutional Ethics Committee and informed consent was obtained from the patients. All cell culture media contained 1% penicillin/streptomycin. The proteins SDF1α (R&D Systems, Minneapolis, MN USA), MCP1 (Invitrogen, San Diego, CA USA), MIP1α (Invitrogen, San Diego, CA USA), and CCN1 (Cell sciences, Canton, MA USA) were used at 200 ng/mL. for stimulation. cRGD peptide (H4772, Bachem, Bubendorf, Switzerland) was used at 10 μM for preincubation.

Development of Adenoviral CCN1 Vectors

A full-length murine CCN1-cDNA was amplified from the expression plasmid pAdTrackCMV as a PCR product by using the primer-linkers mCyr61-1s-EcoRI (5´-cta gaa ttc atg agc tcc agc acc ttc agg acg-3´) and mCyr61-BamHIas (5´-gct gga tcc tta gtc cct gaa ctt gtg ga-3´) which amplify NM_010516 sequence nucleotides 194-1333. This product was directionally cloned into the adenovector transfer plasmid pZS2 digested with EcoRI and BamHI. Subsequently the recombinant plasmid pZS2-mCCN1 was digested with Xba I and ligated to the long arm of the adenovirus strain RR5 as described [1 2]. The ligation product was transfected into HEK293 cells and a recombinant adenoviral clone AdV-CMV-mCCN1 was then amplified and purified by CsCl ultracentrifugation. For the development of the HA-tagged CCN1 vector (HA = hemagglutinin epitope YPYDVPDYA from influenza virus A), CCN1 full-length cDNA was amplified from mouse muscle RNA, after reverse transcription with random primers (*Superscript II, Invitrogen, San Diego, CA USA*), by using the primers #874 mCCN1-forw (5'-cgt cat gaa ttc acc atg agc tcc agc acc ttc ag-3') and #875 mCCN1-rev (5'-cgt cat gtc gac tta gtc cct gaa ctt gtg gat gt-3'). The amplification product was cloned into the pRK5 plasmid. CCN1-HA was then

amplified as a PCR-Product by using the primers #874 mCCN1-forw and #876 mCCN1-HA-rev (5'cgt cat gtc gac tta agc gta gtc tgg gac gtc gta tgg gta gtc cct gaa ctt gtg gat gtc-3') and cloned into pJet1.2 (*Invitrogen, Karlsruhe, Germany*). pJet1.2-mCCN1-HA was digested with EcoRI and Sal I and mCCN1-HA was cloned into pRK5. pRK5-mCCN1-HA was digested with EcoRI and KpnI and CCN1-HA was cloned into the adenovector transfer plasmid pZS2.

CCN1 Vector Evaluation in Cell Cultures

The endothelial Eahy.926 cell line was cultured in 6-well-plates with $5x10^5$ cells per well in 3 mL DMEM medium with Glutamax-I, 10% fetal calf serum, 1% penicillin, 1% streptomycin, and 1xHAT. Cells were transduced after 24h with $3x10^3$ particles of vector AdV-*CMV*-mCCN1 per cell. 72h later cell protein was isolated and culture supernatants collected and both analyzed by Western blot using a polyclonal sheep-anti-mouse-CCN1 primary antibody (*R&D Systems, Minneapolis, MN USA*) in 1:200 dilution and a polyclonal secondary rabbit-anti-sheep-Ig/HRP antibody (*Dako, Glostrup, Denmark*) in 1:1000 dilution. The antibodies detect recombinant mouse CCN1, but not endogenous human Eahy.926-derived or bovine fetal calf serum-derived CCN1. Human and bovine CCN1 were detected instead using a biotinylated polyclonal-goat-anti-CCN1 antibody (*Santa Cruz, Santa Cruz, CA. USA*) in 1:200 dilution at 4°C overnight, followed by streptavidin/HRP conjugate (*Millipore, Billerica, MA USA*) at 1:1000 dilution at room temperature for 1h.

CCN1 Gene Transfer in vivo

For the murine autoimmune myocarditis model, $3x10^{10}$ particles/ mouse of AdV-CMV-mCCN1 or RR5 vector were injected via tail vein into female BALB/c mice 1 week prior to immunization with MyHC-α. AdV-CMV-mCCN1-HA or RR5 vector were injected i.v. in the same doses, into 10 week old mice. For the myocardial infarction (MI) model, AdV-CCN1 or AdV-RR5 were also injected i.v. 4 days prior to MI induction into male C57B/6 mice.

Analysis of Circulating CCN1 Protein

Circulating CCN1 was studied by Western blot of mouse serum proteins after albumin depletion of the serum by ethanol precipitation. To deplete albumin, NaCl was added to ice-cold sera to a concentration of 0.1 M and the samples were then continuously shaken for 60 min. Ice-cold 95%

ethanol was then added to a concentration of 42%. After incubation for 1h at 4°C these samples were centrifuged for 45 min at 13.000 rpm. The pellet was finally re-dissolved with 8M urea /2M thiourea [3]. Circulating CCN1 in heparin plasma of AdV-CCN1-HA-treated, RR5-treated, and non-treated mice was analyzed by ELISA (*DGR Diagnostics, Marburg, Germany*) according to the manufacturer's instructions.

Tracking of Ad-CCN1-HA in vitro and ex vivo

The endothelial Eahy.926 cell line was cultured in 6-well-plates with $3x10^5$ cells per cell in 3 mL DMEM medium with Glutamax-I, 10% fetal calf serum, 1% penicillin, 1% streptomycin, and $3x10^5$ Eahy.926 cells were transduced after 24h with $3x10^3$ particles of vector AdV-*CMV*-mCCN1 per cell. Brefeldin A was added after 48h at 7.5 ng/mL for intracellular staining. After 72h cells were harvested and stained for FACS analysis with anti-HA-FITC antibody (*Miltenyi, Bergisch-Gladbach, Germany*). For FACS analyses, livers, spleens. hearts, and blood PBMCs generated by Ficoll gradient of AdV-CCN1-HA vector-transduced mice and non-transfected control mice were taken on day 25. Single-cell suspensions from all organs were suspended in FACS buffer (PBS supplemented with 2% Flebogamma) and analysed by flow cytometry using a FACS Canto II analyzer (*Beckton Dickinson, Franklin Lakes, NJ USA*) and α-HA-FITC antibody or anti-mouse IgG_1 isotype control (FITC) (*Miltenyi, Bergisch-Gladbach, Germany*). Surface staining was done for extracellular molecules CD11b, CD3e, CD11c, B220, and pan NK cells, respectively *(eBioscience, San Diega, CA USA)*.

Induction of Murine Autoimmune Myocarditis

Vectors were injected i.v. into BALB/c mice (female) one week before their immunization with MyHC-α peptide. Immunization was then conducted by injection of MyHC-α peptide together with CFA, on days 0 and 7. Control mice received 100 µg MyHC-α/CFA only. All analyses were performed at the peak of inflammation occurring 21 days post MyHC-α/CFA immunization. Myocarditis severity score was assessed on hematoxylin-eosin sections and graded from 0 to 4. Histological grading followed a well-established semi-quantitative score from 0 to 4 (0: no inflammatory infiltrates; 1: small foci of inflammatory cells between myocytes; 2: larger foci of 100 inflammatory cells; 3: more than 10% of a cross section involved; and 4: more than 30% of a cross section involved).

Induction and Analysis of Murine Myocardial Infarction

Myocardial infarction (MI) was induced by coronary artery ligation as described [4] and mice were sacrificed 14 days later. Infarction was evident from discoloration of the left ventricle (LV). For histological analysis, hearts were fixed and sectioned (4 µm) and CD45-staining was performed to evaluate the number of leukocytes that had infiltrated the infarcted LV. $CD45^+$ cells in the infarcted area were counted and residual necrotic area (characterized by presence of necrotic cells without evidence of local clearance, collagen deposition, and fibrosis) was calculated planimetrically as percent of this area.

RNA Analyses

The stability of AdV-mCCN1 expression *in vivo* was tested in mouse livers, after i.v. injection of $3x10^{10}$ vector particles/animals (p/a), by Northern blots hybridized with an anti-bGH probe selective for recombinant mCCN1-mRNA over a period of 40 days in mice injected with the vector AdV-mCCN1, RR5, and untreated animals (probe: sense: bgH 134s-NotI: gtt ctt gcg gcc gct tcg ata agc ta; antisense: bgH 418as-XbaI-ClaI-EcoRI: atc tct aga tcg atg ttt gaa tct ccc agc tgg ttc ttt cc). For quantification versus ß-Actin, Scion Image Gelplot2 software (*Scion Corporation, Frederick, MD USA*) was used. Total RNA extraction from mouse hearts, reverse-transcription (RT) reaction and Real Time PCR was performed to analyse the cytokines IFN-γ, IL17A, the chemokines MIP-1α and MCP-1, and the surface molecules CD3 and CD14 (see Supplemental Figure 3), respectively (*Taqman Gene Expression Assay, Applied Biosystems, Foster City, CA USA*). RT PCR was performed for hearts of non-treated mice, mice that received MyHC-α/CFA alone, and mice that received MyHC-α/CFA and either AdV-mCCN1 or RR5 vector. Expression levels were compared to HPRT Expression. Hearts were taken at peak of inflammation.

Migration Assay with Mouse Primary Cells

Single cell suspensions were made from spleens of RR5 transfected and CCN1 transfected BALB/c mice. Erythrocytes were lysed using ACK buffer. Splenocytes were cultured in RPMI 1640 supplemented with 5% FCS, 1% each of penicillin and streptomycin and 2% of glutamin and added to

the upper well of 8 µm Transwell Permeable Supports (*Corning, Corning, NY USA*). Cells were incubated at 37°C, 5% CO_2 for 24h. Cells in lower chamber were harvested, stained for CD11b and CD3e, and resuspended in 100 µL PBS +2% Flebogamma. 30 µL of 1:10 dilution of polystyrol beads *(Comp Beads, neg control, BD, San Diego, CA USA)* were added to each approach. Counting was performed by FACS analysis by gating on the bead population and uptake of exactly 20.000 beads per approach. Counted was the number of cells that were collected in parallel after excluding the bead population. Increase was estimated as ratio to control samples without stimulation. Dead cells were estimated by gating strategy.

Migration Assay with Human Primary Cells and THP-1

PBMCs of healthy human donors (male and female aged 25 to 50) were cultivated in IMDM supplemented with 10% AB serum, 1% each of penicillin and streptomycin. 37°C, 5% CO_2. Lower wells of 96-well transwell (*Corning, Corning, NY USA*) contained 235 µL of IMDM medium +10% AB serum alone or additionally 200 ng/mL MCP-1 (*Invitrogen, San Diego, CA USA*), MIP-1α (*Invitrogen, San Diego, CA USA*) or CCN1 (*Cell sciences, Canton, MA USA*). 75 µL of $1.5x10^5$ PBMCs from healthy human donors purified by Ficoll gradient were suspended in culture medium +10% AB serum and added to the upper well. Cells were incubated at 37°C, 5% CO_2 for 42h. Cells in lower chamber were harvested, stained for CD14 (*BD Pharmingen, San Diego, CA USA)* and proceeded as described before. Furthermore, experiments were done with untouched sorted $CD3^+$ T cells *(CD3 depletion kit, Miltenyi, Bergisch-Gladbach, Germany)* and adhesion enriched CD14 expressing monocytes from human PBMCs. *CCN1 Preincubation*: In pre-incubation experiments cells were stimulated with recombinant human CCN1 for 24h, then washed and re-stimulated as described above. The *in vitro* chemotaxis assay with THP-1 cells was performed as describes for primary cells. Cells in lower chamber were not harvested here, but incubated with MTT (tetrazolium-bromide) 5 mg/mL *(Sigma, Munich, Germany)* in a 1:10 dilution for 4h at 37°C. The 0,04N HCL in isopropanol was added 1:1 into the lower well to dissolve the dark blue crystals. Plates were read at a wavelength of 570 nm against blank without cells and migration was calculated at ratio to unstimulated cells.

Pharmacological Inhibition of CCN1- and Chemokine-Related Signaling Pathways

For the experiments shown in the Supplemental Figure 1 a series of drug inhibitors of cellular signaling pathways was evaluated in THP-1 cells. Acute (black bars "CCN1") *vs* prolonged (grey bars "CCN1 + 24h Pre") CCN1 exposure was compared. Further comparison include Ly294.002, a phosphoinositide 3-kinase (PI3K) inhibitor at 10 μM concentration [5]; Triciribin, an AKT inhibitor at 10 μM [6]; a Rho-kinase inhibitor at 10 μM [7]; PD98059, a MEK inhibitor at 50 μM [5]; a specific inhibitor of PI3Kγ [8]; and two cyclo-RGD peptides (cRGD1, cRGD2) inhibiting αv integrins [9] at 100 μM concentration.

Western Blots

Signal transduction in THP-1 cells was examined by incubation of THP-1 cells for 0 min, 5 min, 30 min, 3h, 8h and 24h either with MCP-1 (*Invitrogen, San Diego, CA USA*) and additionally with 24h CCN1 (*Cell sciences, Canton, MA USA*) preincubation (24h Pre) and afterwards MCP-1 stimulation for indicated time points. Cells were solubilized in general lysis buffer (20 mM Tris, pH 8, 10 mM NaCl, 0.5% (v/v) Triton X-100, 5 mM EDTA, 3 mM MgCl2). After boiling of 30 μg, estimated by BCA method (BCA™ Protein Assay Kit (*Thermo Scientific, Schwerte, Germany*) of the lysate at 95°C for 5 min, proteins were separated on NuPAGE 4–12% Bis–Tris gels (*Invitrogen, San Diego, CA USA*) under denaturing and reducing conditions and transferred to a PVDF membrane (*Bio-Rad, Hercules, CA, USA*). SeeBlue®Plus2 Prestained (*Invitrogen, San Diego, CA USA*) was used as standard. Membranes were incubated with the primary antibodies mouse-α-GAPDH (*Millipore, Billerica, MA USA*), mouse-α-Nck2 1:500 (*Abnova, Neihu District. Taipei City Taiwan*), mouse-α-PINCH 1:1000 (*BD Biosciences* San Diego, CA USA), mouse-α-ILK 1:1000, AKT, and $pAKT^{S472/473}$ (1:500) (*BD Biosciences*, San Diego, CA USA). The primary and the secondary antibody goat-α-mouse Ig-HRP 1:2000 (*Dako, Glostrup, Denmark*) were incubated for 1h or overnight in dry milk. Detection by chemiluminescence was achieved by using an enhanced chemiluminescence system (Rodeo™ ECL Western Blot Detection kit) (*USB Crporation, Cleveland, OH USA*). Quantification versus GAPDH was performed by Scion Image Gelplot2 software (*Scion Corporation, Frederick, MD USA*) (see Supplemental Figure 2).

Chemokine Receptor Expression

PBMCs were either left untreated or stimulated with recombinant human CCN1 protein at 200 ng/mL for 24h. Cells were harvested, stained extracellularly for CCR2, CCR5, and CXCR4, respectively, and analyzed by gating for lymphocyte and monocyte populations by FACS comparing the median fluorescence intensities.

Statistical Analyses

Statistical data analyses were done using the software SPSS 18.0 (SPSS Inc. Chicago, IL USA). Nonparametric statistical methods were used. Continuous variables were expressed as median and interquartile range, if not indicated otherwise. Univariate comparisons of two independent groups were done using the Mann-Whitney-U test. Confirmatory analyses concerning more than two groups were performed by using the Kruskal-Wallis test, followed by *post hoc* testing *via* Mann-Whitney U test with Bonferroni adjustment for multiple testing. To compare between two paired groups, the Wilcoxon sign-rank test was applied. Due to small sample sizes, calculations were done using exact assumption methods (option “exact” in PASW 18.0). A two-tailed p-value of <0.05 was considered statistically significant.

References

1. Suckau L, Fechner H, Chemaly E, Krohn S, Hadri L, Kockskämper J, Westermann D, Bisping E, Ly H, Wang X, Kawase Y, Chen J, Liang L, Sipo I, Vetter R, Weger S, Kurreck J, Erdmann V, Tschope C, Pieske B, Lebeche D, Schultheiss H, Hajjar R, Poller W. Chronic Cardiac-Targeted RNA Interference for the Treatment of Heart Failure Restores Cardiac Function and Reduces Pathological Hypertrophy. *Circulation.* 2009;119:1241-1252.

2. Fechner H, Noutsias M, Tschoepe C, Hinze K, Wang X, Escher F, Pauschinger M, Dekkers D, Vetter R, Paul M, Lamers J, Schultheiss HP, Poller W. Induction of coxsackievirus-adenovirus-receptor expression during myocardial tissue formation and remodeling: identification of a cell-to-cell contact-dependent regulatory mechanism. *Circulation.* 2003;107(6):876-882.

3. Colantonio DA, Dunkinson C, Bovenkamp DE, Van Eyk JE. Effective removal of albumin from serum. *Proteomics.* 2005;5(15):3831-3835.

4. Schellings MW, Vanhoutte D, Swinnen M, Cleutjens JP, Debets J, van Leeuwen RE, d'Hooge J, Van de Werf F, Carmeliet P, Pinto YM, Sage EH, Heymans S. Absence of SPARC results in increased cardiac rupture and dysfunction after acute myocardial infarction. *J Exp Med.*

2009;206(1):113-123.

5. Arefieva TI, Kukhtina NB, Antonova OA, Krasnikova TL. MCP-1-stimulated chemotaxis of monocytic and endothelial cells is dependent on activation of different signaling cascades. *Cytokine.* 2005;31(6):439-446.

6. Dieterle A, Orth R, Daubrawa M, Grotemeier A, Alers S, Ullrich S, Lammers R, Wesselborg S, Stork B. The Akt inhibitor triciribine sensitizes prostate carcinoma cells to TRAIL-induced apoptosis. *Int J Cancer.* 2009;125(4):932-941.

7. Menschikowski M, Hagelgans A, Heyne B, Hempel U, Neumeister V, Goez P, Jaross W, Siegert G. Statins potentiate the IFN-gamma-induced upregulation of group IIA phospholipase A2 in human aortic smooth muscle cells and HepG2 hepatoma cells. *Biochim Biophys Acta.* 2005;1733(2-3):157-171.

8. Camps M, Ruckle T, Ji H, Ardissone V, Rintelen F, Shaw J, Ferrandi C, Chabert C, Gillieron C, Francon B, Martin T, Gretener D, Perrin D, Leroy D, Vitte PA, Hirsch E, Wymann MP, Cirillo R, Schwarz MK, Rommel C. Blockade of PI3Kgamma suppresses joint inflammation and damage in mouse models of rheumatoid arthritis. *Nat Med.* 2005;11(9):936-943.

9. Reynolds AR, Hart IR, Watson AR, Welti JC, Silva RG, Robinson SD, Da Violante G, Gourlaouen M, Salih M, Jones MC, Jones DT, Saunders G, Kostourou V, Perron-Sierra F, Norman JC, Tucker GC, Hodivala-Dilke KM. Stimulation of tumor growth and angiogenesis by low concentrations of RGD-mimetic integrin inhibitors. *Nat Med.* 2009;15(4):392-400.

Supplemental Figures

Supplemental Figure 1

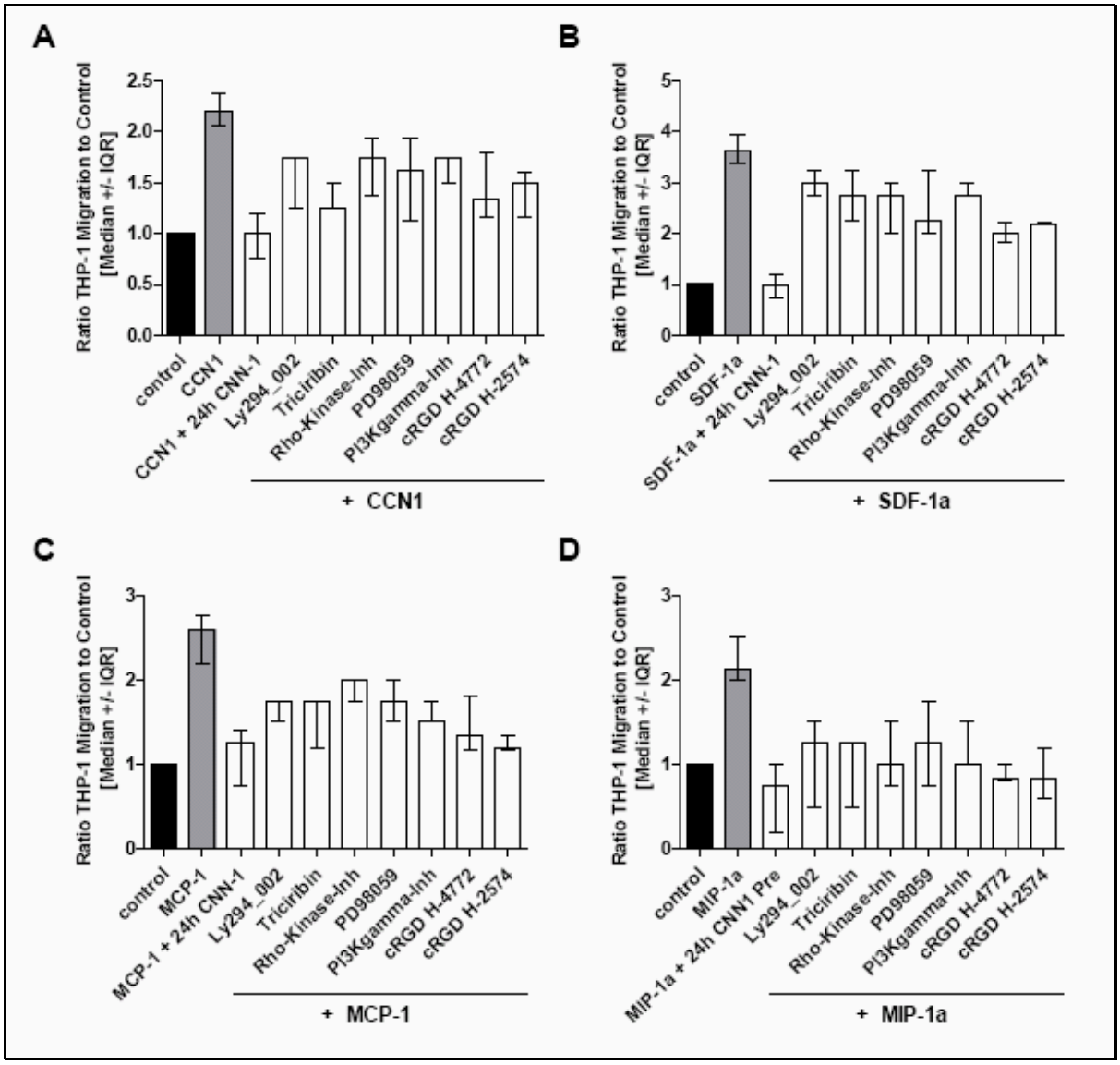

A. Monocytic THP-1 cells were stimulated for 24h either directly with 200 ng/mL of CCN1, (grey bar) or after 1h of pre-incubation with 200 ng/mL CCN1 (CCN1-Pre), the PI3K inhibitor Ly294_002 at 10 μM, PI3Kγ inhibitor at 10 μM, the Akt inhibitor Triciribin at 10 μM, Rho kinase / ROCK inhibitor at 10 μM, MEK inhibitor PD98059 at 50 μM, and cRGD peptide 1 at 100 μM (H4772) and cRGD peptide 2 at 100 μM (H2574), respectively.

B, C, D show the data from analogous experimental settings using stimulation with SDF-1α (panel B), MCP-1 (panel C), or MIP-1α (panel D).

Supplemental Figure 2

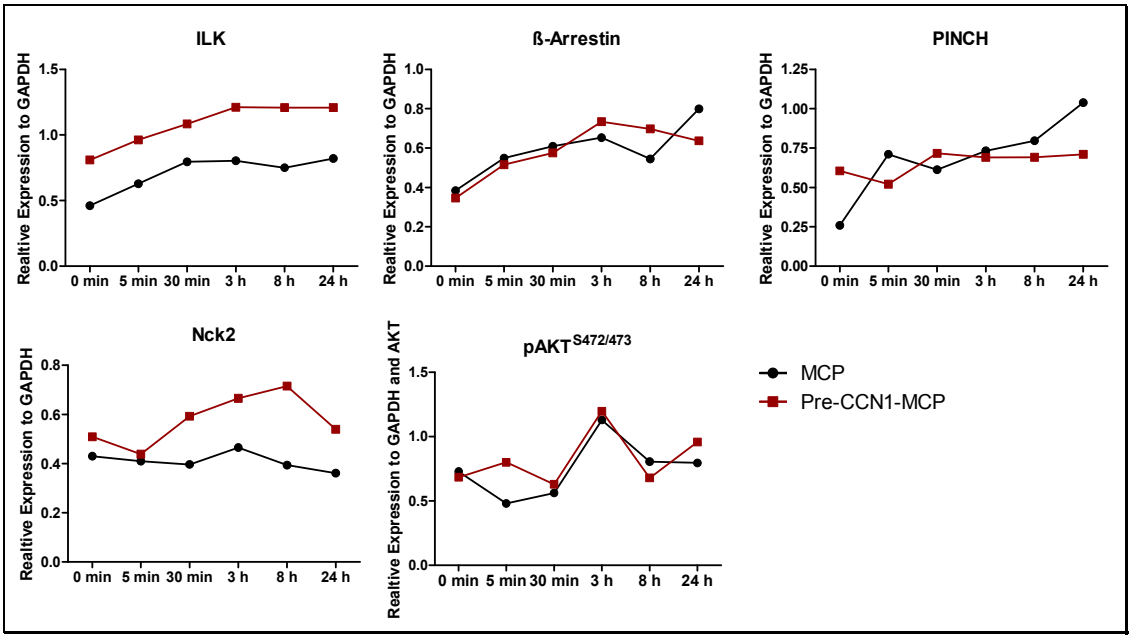

Figure Legend: Intracellular signal transduction proteins linked to integrins and AKT phosphorylation were analyzed by Western blot. The black curves show THP-1 protein expression levels of ILK, NCK2, PINCH, and β-arrestin 2 that blocks G protein-mediated signaling, at various time points (5 min, 30 min , 3h , 8h , and 24h) after addition of 200 ng/mL MCP-1. The red curves show similar analyses, but with addition of the MCP-1 after a preceding preincubation with CCN1 at 200 ng/mL for 24h (shown is one of at least two independent experiments). Protein expression levels of ILK, β-arrestin, PINCH, and Nck2 were referred to GAPDH. Expression level of pAKT$^{S472/472}$ was referred to GAPDH and total AKT, respectively. Quantification was performed by Scion Image Gelplot2 software. Densitometric analysis showed that MCP-1 induced, as expected, upregulation of ILK, β-arrestin, PINCH, and pAKTS$^{472/473}$, but on the other hand detected no inhibitory effect of the 24h-CCN1-preincubation on these inductions.

Supplemental Figure 3

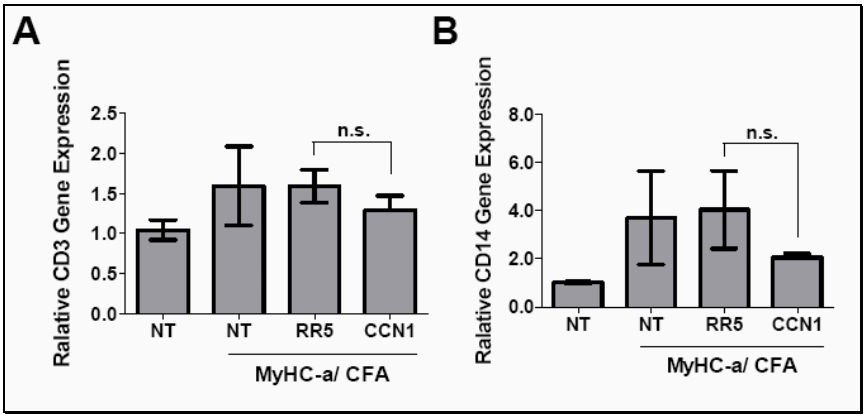

Figure Legend: RT-PCR of mice heart tissues was performed to analyze the surface molecules CD3 (panel A) and CD14 (panel B) characterizing infiltrates of T cells and monocytes/macrophages, respectively. RT-PCR was performed for hearts of non-treated mice (NT), mice that received MyHC-α/CFA alone (NT/MyHC-α/CFA), and mice that received MyHC-α/CFA plus either AdV-CCN1 (CCN1) or RR5 (RR5) vector. The expression levels were compared to HPRT expression. Hearts were taken at the peak of inflammation.